National Library of Canada

Acquisitions and Bibliographic Services Branch

395 Wellington Street
Ottawa, Ontario
K1A 0N4

Bibliothèque nationale du Canada

Direction des acquisitions et des services bibliographiques

395, rue Wellington
Ottawa (Ontario)
K1A 0N4

Your file Votre référence

Our file Notre référence

NOTICE

The quality of this microform is heavily dependent upon the quality of the original thesis submitted for microfilming. Every effort has been made to ensure the highest quality of reproduction possible.

If pages are missing, contact the university which granted the degree.

Some pages may have indistinct print especially if the original pages were typed with a poor typewriter ribbon or if the university sent us an inferior photocopy.

AVIS

La qualité de cette microforme dépend grandement de la qualité de la thèse soumise au microfilmage. Nous avons tout fait pour assurer une qualité supérieure de reproduction.

S'il manque des pages, veuillez communiquer avec l'université qui a conféré le grade.

La qualité d'impression de certaines pages peut laisser à désirer, surtout si les pages originales ont été dactylographiées à l'aide d'un ruban usé ou si l'université nous a fait parvenir une photocopie de qualité inférieure.

Canada

Free Vibration Studies of Shear Deformable Plates By The Traditional Superposition And Superposition-Galerkin Method

Thesis Submitted to the School of Graduate Studies as Partial Fulfilment of the Requirements for the Degree of Master of Applied Science

By

WEI DING

Department of Mechanical Engineering
Ottawa-Carleton Institute for Mechanical and Aerospace Engineering
University of Ottawa
Ottawa, Ontario, Canada

May, 1995

ISBN 0-612-04959-0

Canada

UNIVERSITÉ D'OTTAWA
UNIVERSITY OF OTTAWA

Free Vibration Studies of Shear Deformable Plates By The Traditional Superposition And Superposition-Galerkin Method

Thesis Submitted to the School of Graduate Studies as Partial Fulfilment of the Requirements for the Degree of Master of Applied Science

By

WEI DING

Department of Mechanical Engineering
Ottawa-Carleton Institute for Mechanical and Aerospace Engineering
University of Ottawa
Ottawa, Ontario, Canada

May, 1995

ABSTRACT

In the first part of the present study, it is demonstrated that the traditional superposition method lends itself successfully to obtaining of eigenvalues and mode shapes for completely free shear deformable plates, namely, the thick isotropic plates and symmetric cross-ply laminated plates. The effect of transverse shear deformation is taken into account by means of the first order shear deformation relationship as developed by Mindlin. The governing differential equations are satisfied exactly throughout the plate domain and free edge boundary conditions are satisfied to any desired degree of accuracy. These appear to be the first accurate solutions to these important completely free plate vibration problems.

Subsequently, a new modified Superposition-Galerkin method is developed for analyzing the free vibration problem of symmetric cross-ply plates with any combination of clamped and simply supported boundary conditions. It is shown that this new approach leads to vast simplification of computational procedures in comparison to the traditional superposition method. Nevertheless it is seen that excellent agreement is achieved when results obtained by the Galerkin-Superposition method are compared with those generated by previous researchers. It is expected that this new modified method will have application to various families of laminated plate vibration problems.

ACKNOWLEDGEMENTS

The author would like to express his deep appreciation for the guidance and assistance he has received from his supervisor Dr. D.J. Gorman. Without his years of experience in the field of plate vibration and his countless thoughtful suggestions and ideas, this work would not have been possible.

Special thanks also go to members of the Department of Mechanical Engineering, University of Ottawa, for their support and cooperation.

Finally, the author wishes to thank his wife, Yingping Lai, for her love, patience, understanding and encouragement while this work was being completed.

Contents

ABSTRACT i

ACKNOWLEDGEMENTS ii

NOMENCLATURE v

LIST OF TABLES viii

LIST OF FIGURES x

Chapter 1 Introduction 1

1.1 Literature Survey 1

1.2 Motivation and Objectives 4

Chapter 2 The Underlying Theory 7

2.1 Governing Differential Equations 7

2.2 Boundary Conditions 20

Chapter 3 The Traditional Superposition Method for Analyzing Completely Free Rectangular Plates 25

3.1 Completely Free Isotropic Plates 25

3.1.1 Mathematical Procedures 25

3.1.2 Presentation of Computed Results 42

3.2 Completely Free Symmetric Cross-ply Laminated Plates 44

3.2.1 Mathematical Procedures 44

3.2.2 Presentation of Computed Results 52

Chapter 4 The Superposition-Galerkin Method for Analyzing Rectangular Plates with Combinations of Clamped and Simply supported

Edges Conditions 56

4.1 Mathematical Procedures 57
4.2 Presentation of Computed Results 62

Chapter 5 Summary 66

5.1 Discussion and Conclusions 66
5.2 Further Research Possibilities 69

Reference 71

Appendix I Illustrative Figures 76

Appendix II Computed Eigenvalues and Associated Mode Shapes . . 82

Nomenclature

x,y,z	Cartesian Coordinates
a,b	plate dimensions in x and y directions, respectively
ξ	nondimensional in-plane coordinate, $\xi = x/a$
η	nondimensional in-plane coordinate, $\eta = y/b$
h	plate thickness
ϕ	plate aspect ratio, $\phi = b/a$
ϕ_h	plate thickness-to-length ratio, $\phi_h = h/a$
ρ	plate density per unit area
u,v,w	displacements in x,y and z directions, respectively
W	lateral displacement divided by side length a
ψ_x, ψ_y	rotations with respect to x and y, respectively
ψ_ξ, ψ_η	rotations with respect to ξ and η, respectively
ε_x, ε_y, γ_z	plate strain components
γ_{zx}, γ_{yz}	
σ_x, σ_y, τ_{xy}	plate stress components
τ_{zx}, τ_{yx}	

Q_x, Q_y	shear forces on planes x=const. and y=const. , respectively
Q_ξ, Q_η	corresponding nondimensional shear forces
M_x, M_y, M_{xy}	bending and twisting moments
M_ξ, M_η, $M_{\xi\eta}$	corresponding nondimensional bending and twisting moments
ν	Poisson ratio for isotropic plates
E	Young's modulus for isotropic plates
G	shear modulus for isotropic plates
D	flexural rigidity for isotropic plates, $D = Eh^3/(1-\nu^2)$
D_x, D_y, H	flexural rigidity parameters for orthotropic plates
ν_{12}, ν_{21}	Poisson ratios for individual lamina of laminated plates
G_{12}, G_{23}, G_{31}	shear moduli in three coordinate planes of individual lamina
E_1, E_2	Young's moduli of individual lamina in directions parallel and perpendicular to fibres, respectively
z_k	transverse distance from the upper surface of k-th lamina to the midplane
Q_{ii}	stiffness of individual lamina
A_{ii}	extensional rigidity parameters for laminated plates
a_{ii}	extensional rigidity parameters for laminated plates divided by E_2h
D_{ii}	flexural rigidity parameters for laminated plates
d_{ii}	flexural rigidity parameters for laminated plates divided by E_2h^3
κ^2	shear correction factor
ω	circular frequency of plate free vibration
λ^2	eigenvalues of plate free vibration

for isotropic plates, $\lambda^2 = \omega a^2\sqrt{\rho/D}$

for laminated plates, $\lambda^2 = \omega a^2\sqrt{\rho/E_2h^3}$

K actual number of terms used in series of Levy type solutions

KK actual number of terms used in series of Galerkin techniques

List of Tables

Table A.1 Eigenvalues computed for completely free isotropic thick plates ($\nu = 0.333$; $\kappa^2 = 0.8601$; $\phi = 1.0$)

Table A.2 Eigenvalues computed for completely free isotropic thick plates ($\nu = 0.333$; $\kappa^2 = 0.8601$; $\phi = 1.25$)

Table A.3 Eigenvalues computed for completely free isotropic thick plates ($\nu = 0.333$; $\kappa^2 = 0.8601$; $\phi = 1.5$)

Table A.4 Eigenvalues computed for completely free isotropic thick plates ($\nu = 0.333$; $\kappa^2 = 0.8601$; $\phi = 2.0$)

Table A.5 Eigenvalues computed for completely free isotropic thick plates ($\nu = 0.333$; $\kappa^2 = 0.8601$; $\phi = 2.5$)

Table A.6 Eigenvalues computed for completely free isotropic thick plates ($\nu = 0.333$; $\kappa^2 = 0.8601$; $\phi = 3.0$)

Table A.7 Comparison of eigenvalues, $\lambda^2 = \omega a^2 \sqrt{\rho / E_2 h^3}$, for orthotropic plates with $D_x / D_y = 4.0$, $H = \sqrt{D_x D_y}$, $\sqrt{\nu_{12} \nu_{21}} = 0.25$. T.P.T. and P indicate plate theory [6] and the present theory, respectively. Parameters ϕ_h was set equal to 0.01 .

Table A.8 First four eigenvalues, $\lambda^2 = \omega a^2\sqrt{\rho/E_2h^3}$, for completely free $0^0/90^0/0^0$ symmetric cross-ply plates. Materials properties as given by Khdeir [19]. ($\phi \geq 1$, $\phi_h = 0.1$)

Table A.9 First four eigenvalues, $\lambda^2 = \omega a^2\sqrt{\rho/E_2h^3}$, for completely free $0^0/90^0/0^0$ symmetric cross-ply plates. Materials properties as given by Khdeir [19]. ($1/\phi \geq 1$, $\phi_h = 0.1$)

Table A.10 Comparison of computed eigenvalues, $\lambda^2 = \omega a^2\sqrt{\rho/E_2h^3}$, for square symmetric cross-ply plates ($\phi_h = 0.1$). HSDPT and HSDT results taken from publication of Khdeir [19].

Table A.11 Comparison of computed eigenvalues, $\lambda^2 = \omega a^2\sqrt{\rho/E_2h^3}$, for square symmetric cross-ply plates ($E_1/E_2 = 40.0$). HSDPT and HSDT results taken from publication of Khdeir [19].

Table A.12 First six computed eigenvalues, $\lambda^2 = \omega a^2\sqrt{\rho/E_2h^3}$, for symmetric cross-ply laminated plates with fully clamped boundary conditions. ($\phi_h = 0.1$, $E_1/E_2 = 40.0$)

List of Figures

Figure 1 Schematic representation of forced vibration solutions (building blocks) utilized in free vibration analysis of completely free shear deformable plates

Figure 2 Schematic representation of eigenvalue matrix generated in free vibration analysis of completely free shear deformable plates

Figure 3 Schematic representation of forced vibration solutions (building blocks) superimposed in order to solve the free vibration problem of fully clamped symmetric cross-ply plates

Figure 4 Schematic representation of system of simultaneous non-homogeneous algebraic equations relating coefficients employed in Galerkin method

Figure 5 Schematic representation of eigenvalue matrix generated for solving the free vibration problem of fully clamped symmetric cross-ply plates

Figure A.1 First mode shape of completely free thick isotropic square plates by the traditional superposition method ($\phi_h = 0.1$, $\lambda^2 = 12.44$)

Figure A.2 Second mode shape of completely free thick isotropic square plates by the traditional superposition method ($\phi_h = 0.1$, $\lambda^2 = 18.58$)

Figure A.3 Third mode shape of completely free thick isotropic square plates by the traditional superposition method ($\phi_h = 0.1$, $\lambda^2 = 23.45$)

Figure A.4 First mode shape of completely free symmetric cross-ply square plates by the traditional superposition method ($\phi_h = 0.1$, $\lambda^2 = 4.873$)

Figure A.5 Second mode shape of completely free symmetric cross-ply square plates by the traditional superposition method ($\phi_h = 0.1$, $\lambda^2 = 9.662$)

Figure A.6 Third mode shape of completely free symmetric cross-ply square plates by the traditional superposition method ($\phi_h = 0.1$, $\lambda^2 = 13.33$)

Figure A.7 First mode shape of fully clamped symmetric cross-ply square plates by the Superposition-Galerkin method ($\phi_h = 0.1$, $\lambda^2 = 21.45$)

Figure A.8 Second mode shape of fully clamped symmetric cross-ply square plates by the Superposition-Galerkin method ($\phi_h = 0.1$, $\lambda^2 = 29.98$)

Figure A.9 Third mode shape of fully clamped symmetric cross-ply square plates by the Superposition-Galerkin method ($\phi_h = 0.1$, $\lambda^2 = 40.39$)

Chapter 1

Introduction

1.1 Literature Review

As important structural elements, fibre-reinforced laminated plates with anisotropic mechanical properties, high specific strength (failure stress/unit weight) and high specific stiffness (stiffness/unit weight), find wide application in various fields of engineering, especially in the aerospace industry. They are also more and more used in the automobile industry, for example as car body components, and in the electronic industry as substrate materials for printed circuit boards. Accurate knowledge of their dynamic behaviour is essential in the design of plates made of composite materials.

In recent years, numerous advances have been made in connection with free vibration of

laminated plates, and a wide variety of plate theories as well as analytical techniques have been developed. Many numerical methods, such as the finite element method and the boundary element method, have also been used successfully in this area. It is not the objective of this study to present an all-inclusive bibliography related to this subject. It will be found that the publications to which reference is made already contain such bibliographies. Rather, in this thesis, reference will be made to those publications which are considered to have direct relevance to problems under discussion and their solutions.

It is well known that results obtained by classic plate theory based on the Kirchhoff hypothesis are not truly applicable to plate vibration problems when the plate length-to-thickness ratio falls below certain levels. The Kirchhoff hypothesis assumes that straight lines originally normal to the plate median surface remain straight and normal during the deformation process. This simplifies the problem considerably but produces errors since the effects of transverse shear deformation are neglected. The classic plate theory overestimates the vibration frequencies of thick plates since the plate flexibility is underestimated. This phenomenon was well recognized by many researchers, like Reissner[1], and Mindlin[2]. Many refined plate theories based on discarding the Kirchhoff hypothesis and incorporating transverse shear deformation effects were subsequently developed. It was Mindlin who first developed a mathematical free vibration formulation of the thick plate problem which not only incorporated the effects of deformation associated with transverse shear but also considered the effects of rotary inertia of the plate elements. In the Mindlin plate theory any straight line originally normal to the plate median surface will, during deformation, remain straight but not generally normal to the plate median

surface. In the true situation such a line is generally curved but the assumed straight non-normal line can well approximate this curved line in an average sense at all points. One can think of the work of Mindlin as an extension of the Timoshenko thick beam theory to the two dimensional rectangular plate problem.

Considering laminated plates, one finds that their analysis constitutes a much more complicated problem, even when plates are thin. This is because of the fact that the transverse shear stiffness of such plates is known to be relatively low in comparison to the in-plane stiffness. Accordingly they must be treated as "shear deformable" bodies. The Mindlin plate theory is simple and adequate for free vibration analysis of "shear deformable" plates. A comparison prepared by Yu and Cleghorn[13] indicates that there is excellent agreement between results obtained by using Mindlin plate theory and those of higher order plate theories. Therefore, the Mindlin plate theory is adopted in this study.

The superposition method for free vibration analysis has been used with considerable success to obtain accurate solutions to numerous thin plate free vibration problems. These solutions have been widely reported in the literature with the principal reference being the work of Gorman[3]. An attractive feature of the superposition method centres around the fact that, unlike the Rayleigh-Ritz method which is often employed by many researchers in their papers, no shape functions need to be selected to represent the deformed plate. Exact Levy type solutions are obtained for four rectangular-plate forced vibration problems (building blocks). Each is driven by a harmonic bending moment distributed along one edge. After superimposing these solutions,

Fourier coefficients appearing therein are adjusted in order to satisfy the various boundary conditions. All solutions obtained by the superposition method satisfy the governing differential equations exactly throughout the domain of the plate. The boundary conditions are satisfied to any desired degree of accuracy.

More recently, the superposition method has been employed by Yu and Cleghorn[15] to analyze Mindlin plates and laminated plates with combinations of clamped and simply supported edge conditions. Li and Mirza[30] solved free vibration problems for laminated orthotropic plates and shells by combined superposition method and state-space technique. Many other researchers also made significant contributions to studies in the free vibration of plates. For further investigation, one is referred to the papers and books by Leissa[24,25,26], Reddy[27,28], Bert[32,33,34] and so on.

1.2 Motivation and Objectives

It is noted that analytical solutions for thick isotropic plates or laminated plates are not only scarce but are available mostly for plates with clamped and simply supported boundary conditions, and it is well known that researchers tend to avoid completely free plate problems because of the traditional difficulties related to handling the free edge conditions.

In the first part of this thesis, the traditional superposition method is exploited to obtain solutions for the natural frequencies and mode shapes of completely free thick isotropic and laminated plates. To the author's knowledge, those solutions represent the first accurate solutions to be achieved for these challenging problems.

There is no doubt that the traditional superposition method provides a powerful means for analyzing free vibration problems of rectangular plates. It also remains a fact, nevertheless, that as one moves away from thin isotropic plates towards thick plates or laminated plates, where the effects of transverse shear deformation can no longer be neglected, the exploitation of even the traditional superposition method becomes more and more challenging. This difficulty arises mainly because of the large number of combinations of complex, real and imaginary roots which are encountered when one examines the characteristic equations associated with the building blocks of these more complicated problems. In a typical approach one obtains a separation of variables, but now this leads to a high order ordinary differential equation and hence the high order characteristic equation with numerous possible combinations of roots, depending on the equation coefficients. It is also known that due to the presence of hyperbolic functions in the classic type solutions encountered when utilizing the superposition method, computer overflow or underflow problems and even computational instability may be experienced.

In the second part of this thesis, a new modified Superposition-Galerkin method is introduced. It is shown how all of the benefits of the superposition technique may be retained while all of the computational problems of searching for multi roots of equations as well as

computer overflow or underflow problems may be avoided by exploitation of this new method. The details of the modified Superposition-Galerkin method are illustrated hereinafter. Excellent agreement is achieved between the results obtained by the Superposition-Galerkin method and those reported in the published literature. Rapid convergence is obtained. It will be seen that the Superposition-Galerkin method is much more straight forward and advantages of this method become more pronounced as problems become more complicated.

Chapter 2

The Underlying Theory

In this chapter, the dimensionless governing differential equations for free vibration analysis of thick isotropic and laminated plates, based on Mindlin plate theory, are developed for the sake of completeness. Also, the associated various boundary conditions will be presented.

2.1 Governing Differential Equations

2.1.1 Governing Differential Equations for Thick Isotropic Plates

The rectangular plate is referred to an x,y,z system of rectangular coordinates. The faces of the plate are the planes $z = \pm h/2$. The notation for plate stress and strain components as well as materials properties are defined in customary manner [2].

Consider the general Hooke's law for isotropic materials in three-dimensional elasticity theory with the expressions for the six components of strain in term of six components of stress. Of the six equations, the one containing unit elongation, ε_z , normal to the faces of the plate is dropped, and σ_z is also neglected. The remaining five equations are then solved for stress components σ_x , σ_y , τ_{xy} , τ_{zx} , τ_{yz} in terms of strain components ε_x , ε_y , γ_{xy} , γ_{zx} , γ_{yz} . One arrives at the plate stress-strain relationship.

$$\sigma_x = \frac{E}{1-\nu^2}\,(\varepsilon_x + \nu\varepsilon_y)$$

$$\sigma_y = \frac{E}{1-\nu^2}\,(\varepsilon_y + \nu\varepsilon_x)$$

$$\tau_{xy} = G\gamma_{xy} \qquad (2.1)$$

$$\tau_{zx} = G\gamma_{zx}$$

$$\tau_{yz} = G\gamma_{yz}$$

From the three-dimensional elasticity theory, we also have the following plate strain-displacement relationships by ignoring the equation containing strain ε_z .

$$\varepsilon_x = \frac{\partial u}{\partial x}$$

$$\varepsilon_y = \frac{\partial v}{\partial y}$$

$$\gamma_{xy} = \frac{\partial u}{\partial y} + \frac{\partial v}{\partial x} \qquad (2.2)$$

$$\gamma_{zx} = \frac{\partial u}{\partial z} + \frac{\partial w}{\partial x}$$

$$\gamma_{yz} = \frac{\partial w}{\partial y} + \frac{\partial v}{\partial z}$$

where u, v, and w are plate displacements in x, y, and z directions, respectively.

The plate bending and twisting moments and transverse shear forces, all per unit of length, are now defined as follows

$$M_x = \int_{-h/2}^{h/2} \sigma_x z \, dz$$

$$M_y = \int_{-h/2}^{h/2} \sigma_y z \, dz$$

$$M_{xy} = \int_{-h/2}^{h/2} \tau_{xy} z \, dz \qquad (2.3)$$

$$Q_x = \int_{-h/2}^{h/2} \tau_{zx} \, dz$$

$$Q_y = \int_{-h/2}^{h/2} \tau_{yz}\, dz$$

It is assumed in the Mindlin theory that u and v are proportional to z and w is independent of z

$$\begin{aligned} u &= z\,\psi_x(x, y, t) \\ v &= z\,\psi_y(x, y, t) \\ w &= w(x, y, t) \end{aligned} \tag{2.4}$$

where ψ_x and ψ_y are the local rotations (change of slope) in the x and y directions, respectively, of lines originally normal to the plate before deformation.

Substituting equations (2.4) into strain-displacement equations (2.2), then into stress-strain equations (2.1), one obtains

$$\begin{aligned} \sigma_x &= \frac{Ez}{1-\nu^2}\left(\frac{\partial \psi_x}{\partial x} + \nu\frac{\partial \psi_y}{\partial y}\right) \\ \sigma_y &= \frac{Ez}{1-\nu^2}\left(\frac{\partial \psi_y}{\partial y} + \nu\frac{\partial \psi_x}{\partial x}\right) \\ \tau_{xy} &= \frac{Ez}{2(1+\nu)}\left(\frac{\partial \psi_x}{\partial y} + \frac{\partial \psi_y}{\partial x}\right) \end{aligned} \tag{2.5}$$

$$\tau_{xz} = G\left(\psi_x + \frac{\partial w}{\partial x}\right)$$

$$\tau_{yz} = G\left(\psi_y + \frac{\partial w}{\partial y}\right)$$

The first three equations of equations (2.5) are multiplied by z and integrated over the plate thickness, the last two equations of equations (2.5) are integrated over plate thickness directly. One finally achieves, after incorporating equations (2.3), the expressions for bending and twisting moments and shear forces in terms of plate displacements.

$$M_x = D\left(\frac{\partial \psi_x}{\partial x} + \nu \frac{\partial \psi_y}{\partial y}\right)$$

$$M_y = D\left(\frac{\partial \psi_y}{\partial y} + \nu \frac{\partial \psi_x}{\partial x}\right)$$

$$M_{xy} = \frac{1-\nu}{2} D\left(\frac{\partial \psi_y}{\partial x} + \frac{\partial \psi_x}{\partial y}\right) \qquad (2.6)$$

$$Q_x = \kappa^2 G h \left(\psi_x + \frac{\partial w}{\partial x}\right)$$

$$Q_y = \kappa^2 G h \left(\psi_y + \frac{\partial w}{\partial y}\right)$$

where D is the plate modulus

$$D = Eh^3 / 12\left(1-\nu^2\right) \qquad (2.7)$$

and κ^2 is the constant, introduced here as transverse shear correction coefficient.

Now consider the well-known stress equations of motion of three-dimensional elasticity theory

$$\frac{\partial \sigma_x}{\partial x} + \frac{\partial \tau_{xy}}{\partial y} + \frac{\partial \tau_{zx}}{\partial z} = \frac{\rho}{h} \frac{\partial^2 u}{\partial t^2}$$

$$\frac{\partial \tau_{xy}}{\partial x} + \frac{\partial \sigma_y}{\partial y} + \frac{\partial \tau_{yz}}{\partial z} = \frac{\rho}{h} \frac{\partial^2 v}{\partial t^2} \qquad (2.8)$$

$$\frac{\partial \tau_{xz}}{\partial x} + \frac{\partial \tau_{yz}}{\partial y} + \frac{\partial \sigma_z}{\partial z} = \frac{\rho}{h} \frac{\partial^2 w}{\partial t^2}$$

where ρ is the density per unit area.

The first two equations of equations (2.8) are multiplied by z and integrated over the plate thickness, and the third equation of equations (2.8) is integrated over the plate thickness directly. After making use of equations (2.3), (2.4) and the condition that the plate is free of inplane forces, transverse external loading or body forces, and neglecting the stress σ_z , equations (2.8) becomes

$$\frac{\partial M_x}{\partial x} + \frac{\partial M_{xy}}{\partial y} - Q_x = \frac{\rho h^2}{12} \frac{\partial^2 \psi_x}{\partial t^2}$$

$$\frac{\partial M_{xy}}{\partial x} + \frac{\partial M_y}{\partial y} - Q_y = \frac{\rho h^2}{12} \frac{\partial^2 \psi_y}{\partial t^2} \qquad (2.9)$$

$$\frac{\partial Q_x}{\partial x} + \frac{\partial Q_y}{\partial y} = \rho \frac{\partial^2 w}{\partial t^2}$$

Substituting equations (2.6) into equations (2.9), one finally gets the governing differential equations for Mindlin plates

$$\kappa^2 G h \left(\frac{\partial^2 w}{\partial x^2} + \frac{\partial^2 w}{\partial y^2} + \frac{\partial \psi_x}{\partial x} + \frac{\partial \psi_y}{\partial y} \right) = \rho \frac{\partial^2 w}{\partial t^2}$$

$$\frac{D}{2} \left[2 \frac{\partial^2 \psi_x}{\partial x^2} + (1-\nu) \frac{\partial^2 \psi_x}{\partial y^2} + (1+\nu) \frac{\partial^2 \psi_y}{\partial x \partial y} \right]$$

$$-\kappa^2 G h \left(\psi_x + \frac{\partial w}{\partial x} \right) = \frac{\rho h^2}{12} \frac{\partial^2 \psi_x}{\partial t^2} \qquad (2.10)$$

$$\frac{D}{2} \left[2 \frac{\partial^2 \psi_y}{\partial y^2} + (1-\nu) \frac{\partial^2 \psi_y}{\partial x^2} + (1+\nu) \frac{\partial^2 \psi_x}{\partial x \partial y} \right]$$

$$-\kappa^2 G h \left(\psi_y + \frac{\partial w}{\partial y} \right) = \frac{\rho h^2}{12} \frac{\partial^2 \psi_y}{\partial t^2}$$

It is possible to express the displacement w(x,y,t), edge rotations ψ_x (x,y,t) and ψ_y (x,y,t) as a product of two functions, respectively, one involving only the space coordinate x and y and the other involving the time variable,

$$\begin{aligned} w(x,y,t) &= w'(x,y)\, T(t) \\ \psi_x(x,y,t) &= \psi_x'(x,y)\, T(t) \\ \psi_y(x,y,t) &= \psi_y'(x,y)\, T(t) \end{aligned} \qquad (2.11)$$

Substituting equations (2.11) into equations (2.10), it can be shown that

$$T(t) = A\sin(\omega t + \alpha) \tag{2.12}$$

where ω is known as circular frequency, A and α represent the amplitude and the phase angle, respectively. For the sake of brevity, w, ψ_x and ψ_y will again be used hereafter to represent the space functions, $w'(x,y)$, $\psi_x'(x,y)$ and $\psi_y'(x,y)$. The equations (2.10) then become

$$\kappa^2 G h \left(\frac{\partial^2 w}{\partial x^2} + \frac{\partial^2 w}{\partial y^2} + \frac{\partial \psi_x}{\partial x} + \frac{\partial \psi_y}{\partial y}\right) + \rho\,\omega^2 w = 0$$

$$\frac{D}{2}\left[2\frac{\partial^2 \psi_x}{\partial x^2} + (1-\nu)\frac{\partial^2 \psi_x}{\partial y^2} + (1+\nu)\frac{\partial^2 \psi_y}{\partial x\,\partial y}\right]$$

$$-\kappa^2 G h \left(\psi_x + \frac{\partial w}{\partial x}\right) + \frac{\rho\omega^2 h^2}{12}\psi_x = 0 \tag{2.13}$$

$$\frac{D}{2}\left[2\frac{\partial^2 \psi_y}{\partial y^2} + (1-\nu)\frac{\partial^2 \psi_y}{\partial x^2} + (1+\nu)\frac{\partial^2 \psi_x}{\partial x\,\partial y}\right]$$

$$-\kappa^2 G h \left(\psi_y + \frac{\partial w}{\partial y}\right) + \frac{\rho\omega^2 h^2}{12}\psi_y = 0$$

Experience has shown that it is always advantageous to use the nondimensional governing differential equations. After introducing the following transformations [13],

$$\xi = \frac{x}{a}; \qquad M_\xi = M_x a / D;$$

$$\eta = \frac{y}{b}; \qquad M_\eta = M_y b / D$$

$$W(\xi,\eta) = w(x,y)/a; \qquad M_{\xi\eta} = 2M_{xy} a / D(1-\nu); \tag{2.14}$$

$$\psi_\xi = \psi_x \; ; \qquad Q_\xi = Q_x / \kappa^2 G h$$

$$\psi_\eta = \psi_y \; ; \qquad Q_\eta = Q_y / \kappa^2 G h$$

The nondimensional governing differential equations for Mindlin plates may be written as

$$\frac{\partial^2 W}{\partial \xi^2} + \frac{1}{\phi^2}\frac{\partial^2 W}{\partial \eta^2} + \frac{\partial \psi_\xi}{\partial \xi} + \frac{1}{\phi}\frac{\partial \psi_\eta}{\partial \eta} + \frac{\lambda^4 \phi_h^2}{\nu_3} W = 0$$

$$\frac{\partial^2 \psi_\xi}{\partial \xi^2} + \frac{\nu_1}{\phi^2}\frac{\partial^2 \psi_\xi}{\partial \eta^2} + \frac{\nu_2}{\phi \nu_1}\frac{\partial^2 \psi_\eta}{\partial \xi \partial \eta}$$

$$- \frac{\nu_3}{\phi_h^2}\left(\psi_\xi + \frac{\partial W}{\partial \xi}\right) + \frac{\lambda^4 \phi_h^2}{12}\psi_\xi = 0 \qquad (2.15)$$

$$\frac{\partial^2 \psi_\eta}{\partial \xi^2} + \frac{1}{\phi^2 \nu_1}\frac{\partial^2 \psi_\eta}{\partial \eta^2} + \frac{\nu_2}{\phi \nu_1}\frac{\partial^2 \psi_\xi}{\partial \xi \partial \eta}$$

$$- \frac{\nu_3}{\phi_h^2 \nu_1}\left(\psi_\eta + \frac{1}{\phi}\frac{\partial W}{\partial \eta}\right) + \frac{\lambda^4 \phi_h^2}{12 \nu_1}\psi_\eta = 0$$

where $\phi_h = h/a$, $\nu_1 = (1-\nu)/2$, $\nu_2 = (1+\nu)/2$, $\nu_3 = 6\kappa^2(1+\nu)$, and λ^2 is the eigenvalue,

$$\lambda^2 = \omega a^2 \sqrt{\rho / D} \qquad (2.16)$$

The corresponding nondimensional shearing forces, bending and twisting moments become

$$M_\xi = \frac{\partial \psi_\xi}{\partial \xi} + \frac{\nu}{\phi}\frac{\partial \psi_\eta}{\partial \eta}$$

$$M_\eta = \frac{\partial \psi_\eta}{\partial \eta} + \nu\phi\frac{\partial \psi_\xi}{\partial \xi}$$

$$M_{\xi\eta} = \frac{1}{\phi}\frac{\partial \psi_\xi}{\partial \eta} + \frac{\partial \psi_\eta}{\partial \xi} \qquad (2.17)$$

$$Q_\xi = \psi_\xi + \frac{\partial W}{\partial \xi}$$

$$Q_\eta = \psi_\eta + \frac{1}{\phi}\frac{\partial W}{\partial \eta}$$

2.1.2 Governing Differential Equations for Symmetric Cross-ply Laminated Plates

Consider a plate which is symmetrically laminated by N orthotropic laminae with uniform thickness. Following the conventional notations, for the orthotropic laminae, we have stress-strain relations [17]

$$\begin{aligned}
\sigma_x &= Q_{11}\varepsilon_x + Q_{12}\varepsilon_y \\
\sigma_y &= Q_{12}\varepsilon_x + Q_{22}\varepsilon_y \\
\tau_{xy} &= Q_{66}\gamma_{xy} \qquad (2.18) \\
\tau_{zx} &= Q_{55}\gamma_{zx} \\
\tau_{yz} &= Q_{44}\gamma_{yz}
\end{aligned}$$

where

$$Q_{11} = E_1/(1-\nu_{12}\nu_{21}) \; ; \qquad Q_{22} = E_2/(1-\nu_{12}\nu_{21}) \; ;$$
$$Q_{12} = \nu_{12}E_2/(1-\nu_{12}\nu_{21}) \; ; \qquad Q_{66} = G_{12} \; ; \qquad (2.19)$$
$$Q_{55} = G_{31} \; ; \qquad Q_{44} = G_{23} \; ;$$

and E_1 , E_2 are Young's moduli in x and y direction, respectively, ν_{12} and ν_{21} are Poisson ratios, G_{12} , G_{23} and G_{31} are shear moduli.

From equations (2.2), (2.3), (2.4) and (2.18), after integrating over the plate thickness, one has the expressions for bending and twisting moments and shear forces of the laminated plate in terms of the plate displacements.

$$M_x = D_{11}\frac{\partial \psi_x}{\partial x} + D_{12}\frac{\partial \psi_y}{\partial y}$$

$$M_y = D_{22}\frac{\partial \psi_y}{\partial y} + D_{12}\frac{\partial \psi_x}{\partial x}$$

$$M_{xy} = D_{66}\left(\frac{\partial \psi_x}{\partial y} + \frac{\partial \psi_y}{\partial x}\right) \qquad (2.20)$$

$$Q_x = \kappa^2 A_{55}\left(\psi_x + \frac{\partial w}{\partial x}\right)$$

$$Q_y = \kappa^2 A_{44}\left(\psi_y + \frac{\partial w}{\partial y}\right)$$

where

$$D_{ij} = \frac{1}{3}\sum_{k=1}^{N} (Q_{ij})_k (z_k^3 - z_{k-1}^3) \qquad i,j = 1, 2, 6$$

$$A_{ij} = \kappa^2 \sum_{k=1}^{N} (Q_{ij})_k (z_k - z_{k-1}) \qquad i,j = 4, 5 \tag{2.21}$$

and z_k is the transverse distance from the upper surface of k-th lamina to the midplane. For symmetric cross-ply laminated plates, D_{16}, D_{26} and A_{45} are all zero.

Similarly substituting equations (2.20) into equations (2.9), and separating the time variable from plate displacement variables, one finally obtains the governing differential equations for symmetrically cross-ply laminated plates

$$\kappa^2 A_{55}\left(\frac{\partial \psi_x}{\partial x} + \frac{\partial^2 w}{\partial x^2}\right) + \kappa^2 A_{44}\left(\frac{\partial \psi_y}{\partial y} + \frac{\partial^2 w}{\partial y^2}\right) + \rho\,\omega^2\, w = 0$$

$$D_{11}\frac{\partial^2 \psi_x}{\partial x^2} + D_{66}\frac{\partial^2 \psi_x}{\partial y^2} + (D_{12} + D_{66})\frac{\partial^2 \psi_y}{\partial x\,\partial y}$$

$$-\kappa^2 A_{55}\left(\psi_x + \frac{\partial w}{\partial x}\right) + \frac{\rho\omega^2 h^2}{12}\psi_x = 0 \tag{2.22}$$

$$D_{22}\frac{\partial^2 \psi_y}{\partial y^2} + D_{66}\frac{\partial^2 \psi_y}{\partial x^2} + (D_{12} + D_{66})\frac{\partial^2 \psi_x}{\partial x\,\partial y}$$

$$-\kappa^2 A_{44}\left(\psi_y + \frac{\partial w}{\partial y}\right) + \frac{\rho\omega^2 h^2}{12}\psi_y = 0$$

To nondimensionalize the above three equations, the following transformations are taken

$$\xi = x/a \; ; \qquad M_\xi = M_x a/D_{11} \; ;$$

$$\eta = y/b \; ; \qquad M_\eta = M_y b/D_{22} \; ;$$

$$W(\xi,\eta) = w(x,y)/a \; ; \qquad M_{\xi\eta} = M_{xy} a/D_{66} \; ; \qquad (2.23)$$

$$\psi_\xi = \psi_x \; ; \qquad Q_\xi = Q_x/A_{55} \; ;$$

$$\psi_\eta = \psi_y \; ; \qquad Q_\eta = Q_y/A_{44} \; ;$$

The governing differential equations in nondimensional form may now be written as

$$\kappa^2 a_{55}\left(\frac{\partial \psi_\xi}{\partial \xi} + \frac{\partial^2 W}{\partial \xi^2}\right) + \kappa^2 a_{44}\left(\frac{\partial \psi_\eta}{\partial \eta} + \frac{1}{\phi}\frac{\partial^2 W}{\partial \eta^2}\right) + \lambda^4 \phi_h^2 W = 0$$

$$d_{11}\frac{\partial^2 \psi_\xi}{\partial \xi^2} + \frac{d_{66}}{\phi^2}\frac{\partial^2 \psi_\xi}{\partial \eta^2} + \frac{(d_{12}+d_{66})}{\phi}\frac{\partial^2 \psi_\eta}{\partial \xi \partial \eta}$$

$$-\frac{\kappa^2 a_{55}}{\phi_h^2}\left(\psi_\xi + \frac{\partial W}{\partial \xi}\right) + \frac{\lambda^4 \phi_h^2}{12}\psi_\xi = 0 \qquad (2.24)$$

$$\frac{d_{22}}{\phi^2}\frac{\partial^2 \psi_\eta}{\partial \eta^2} + d_{66}\frac{\partial^2 \psi_\eta}{\partial \xi^2} + \frac{(d_{12}+d_{66})}{\phi}\frac{\partial^2 \psi_\xi}{\partial \xi \partial \eta}$$

$$-\frac{\kappa^2 a_{44}}{\phi_h^2}\left(\psi_\eta + \frac{\partial W}{\partial \eta}\right) + \frac{\lambda^4 \phi_h^2}{12}\psi_\eta = 0$$

where

$$d_{ij} = D_{ij}/E_2 h^3 \qquad \text{i,j} = 1, 2, 6$$

$$a_{ij} = A_{ij} / E_2 h \qquad i,j = 4, 5 \qquad (2.25)$$

$$\lambda^2 = \omega a^2 \sqrt{\rho / E_2 h^3}$$

and the corresponding plate nondimensional bending and twisting moments, and shear force may be written as

$$M_\xi = \frac{\partial \psi_\xi}{\partial \xi} + \frac{d_{12}}{\phi d_{11}} \frac{\partial \psi_\eta}{\partial \eta}$$

$$M_\eta = \frac{\partial \psi_\eta}{\partial \eta} + \frac{\phi d_{12}}{d_{22}} \frac{\partial \psi_\xi}{\partial \xi}$$

$$M_{\xi\eta} = \frac{1}{\phi} \frac{\partial \psi_\xi}{\partial \eta} + \frac{\partial \psi_\eta}{\partial \xi} \qquad (2.26)$$

$$Q_\xi = \psi_\xi + \frac{\partial W}{\partial \xi}$$

$$Q_\eta = \psi_\eta + \frac{1}{\phi} \frac{\partial W}{\partial \eta}$$

2.2 Boundary Conditions

Four types of classic boundary conditions in their dimensionless form, that have been studied thoroughly in the literature, for example Gorman [3], are presented here. In all the

following expressions of boundary conditions, we take those on the edge x = a or $\xi = 1$ as an illustrative example.

2.2.1 Simply Supported Edges

For a simply supported edge at $\xi = 1$, we have

$$\begin{aligned} W &= 0 \\ \psi_\eta &= 0 \\ M_\xi &= 0 \end{aligned} \tag{2.27}$$

Considering equations (2.17) and (2.26) for isotropic plates and symmetric cross-ply laminated plates, respectively, the third condition becomes

$$M_\xi = \frac{\partial \psi_\xi}{\partial \xi} = 0 \tag{2.28}$$

Hence the boundary conditions for a simply supported edge at $\xi = 1$ are

$$\begin{aligned} W &= 0 \\ \psi_\eta &= 0 \\ \partial \psi_\xi / \partial \xi &= 0 \end{aligned} \tag{2.29}$$

2.2.2 Clamped Edges

The boundary conditions for a clamped edge at $\xi = 1$ are

$$\begin{aligned} W &= 0 \\ \psi_\xi &= 0 \\ \psi_\eta &= 0 \end{aligned} \tag{2.30}$$

2.2.3 Free Edges

For a free edge at $\xi = 1$, we have

$$\begin{aligned} M_\xi &= 0 \\ M_{\xi\eta} &= 0 \\ Q_\xi &= 0 \end{aligned} \tag{2.31}$$

In the case of isotropic plates, using equations (2.17), these conditions become

$$\begin{aligned} \frac{\partial \psi_\xi}{\partial \xi} + \frac{\nu}{\phi}\frac{\partial \psi_\eta}{\partial \eta} &= 0 \\ \frac{1}{\phi}\frac{\partial \psi_\xi}{\partial \eta} + \frac{\partial \psi_\eta}{\partial \xi} &= 0 \end{aligned} \tag{2.32}$$

$$\psi_\xi + \frac{\partial W}{\partial \xi} = 0$$

In the case of symmetric cross-ply laminates, using equations (2.26), these conditions become

$$\frac{\partial \psi_\xi}{\partial \xi} + \frac{d_{12}}{\phi d_{11}} \frac{\partial \psi_\eta}{\partial \eta} = 0$$

$$\frac{1}{\phi} \frac{\partial \psi_\xi}{\partial \eta} + \frac{\partial \psi_\eta}{\partial \xi} = 0 \qquad (2.33)$$

$$\psi_\xi + \frac{\partial W}{\partial \xi} = 0$$

2.2.4 Slip Shear Edges

The slip shear support requires that the edge is free of transverse shear forces and twisting moments. In addition, the plate cross section lying along such a boundary, cannot rotate about an axis parallel to the edge. This kind of boundary condition is of a type that would rarely be encountered along the edges of an actual plate. Nevertheless, it will serve as a valuable mathematical device in analyzing plate vibration problems by the superposition method. For a slip shear edge at $\xi = 1$, we have

$$\psi_\xi = 0$$
$$Q_\xi = 0 \qquad (2.34)$$
$$M_{\xi\eta} = 0$$

Incorporating equations (2.17) and (2.26) for isotropic plates and symmetric cross-ply plates, respectively, these boundary conditions become

$$\psi_\xi = 0$$
$$\frac{\partial W}{\partial \xi} = 0 \qquad (2.35)$$
$$\frac{1}{\phi}\frac{\partial \psi_\xi}{\partial \eta} + \frac{\partial \psi_\eta}{\partial \xi} = 0$$

Chapter 3

The Traditional Superposition Method for Analyzing Completely Free Rectangular Plates

In chapter 2, we developed the governing differential equations (2.15) and (2.24) for isotropic thick plates and symmetric cross-ply laminated plates, respectively. We now exploit the traditional superposition method to obtain accurate solutions for the natural frequencies and mode shapes of these plates with completely free edges.

3.1 Completely Free Isotropic Thick Plates

3.1.1 Mathematical Procedure

The governing differential equations for isotropic thick plates are those developed in

chapter 2, equations (2.15). In order to obtain a solution for the completely free plate problem four building blocks (forced vibration problem solutions) are employed. They are represented schematically in Figure 1.

We begin by focusing attention on the first building block. It is subjected to a harmonic edge rotation distributed along the edge, $\eta = 1$. The amplitude of this distributed edge rotation is expressed in series form as

$$\psi_\eta = \sum_{m=0,1}^{\infty} E_m \cos m\pi\xi \tag{3.1}$$

In addition, this driven edge is free of transverse shear stress and twisting moment. The three non-driven edges of this building block are given slip-shear support. This type of support is indicated in the figure by two small circles adjacent to the edge.

One has the option here of driving building blocks instead with a distributed harmonic bending moment. It is found preferable to utilize distributed harmonic edge rotation when analyzing plates with free edges. One thereby avoids the problem of uncovering false eigenvalues (rejection mode eigenvalues) as discussed by Gorman [3].

Levy type solutions are obtained for each of the dependent variables, W, ψ_ξ and ψ_η . The trigonometric functions in the following expressions are selected so that the boundary conditions at extremities of their arguments will be satisfied, as required by Levy solution. We therefore

write,

$$W(\xi,\eta) = \sum_{m=0,1}^{\infty} X_m(\eta)\cos m\pi\xi \tag{3.2}$$

$$\psi_\xi(\xi,\eta) = \sum_{m=1,2}^{\infty} Y_m(\eta)\sin m\pi\xi \tag{3.3}$$

$$\psi_\eta(\xi,\eta) = \sum_{m=0,1}^{\infty} Z_m(\eta)\cos m\pi\xi \tag{3.4}$$

The next step required is to substitute the above expressions for the plate lateral displacement, and slope functions, into the governing differential equations, (2.15). One then obtains, for $m \geq 1$, the following set of coupled ordinary homogenous differential equations which are written in matrix form as

$$\begin{Bmatrix} X_m'' \\ Y_m'' \\ Z_m'' \end{Bmatrix} + \begin{bmatrix} 0 & 0 & a_{m1} \\ 0 & 0 & a_{m2} \\ a_{m3} & a_{m4} & 0 \end{bmatrix} \begin{Bmatrix} X_m' \\ Y_m' \\ Z_m' \end{Bmatrix} + \begin{bmatrix} b_{m1} & b_{m2} & 0 \\ b_{m3} & b_{m4} & 0 \\ 0 & 0 & b_{m5} \end{bmatrix} \begin{Bmatrix} X_m \\ Y_m \\ Z_m \end{Bmatrix} = \begin{Bmatrix} 0 \\ 0 \\ 0 \end{Bmatrix} \tag{3.5}$$

where the primes indicate differentiation with respect to the variable η .

Performing the above substitution, it is found that, for the problem under study, the matrix elements become

$$a_{m1} = \phi$$

$$a_{m2} = -\phi\nu_2(m\pi)/\nu_1 \qquad (3.6)$$

$$a_{m3} = -\nu_3\phi/\phi_h^2$$

$$a_{m4} = \nu_2\phi(m\pi)$$

and

$$b_{m1} = [\frac{\lambda^4\phi_h^2}{\nu_3} - (m\pi)^2]\phi^2$$

$$b_{m2} = (m\pi)\phi^2$$

$$b_{m3} = \frac{\nu_3\phi^2(m\pi)}{\nu_1\phi_h^2} \qquad (3.7)$$

$$b_{m4} = \frac{\phi^2}{\nu_1}[\frac{\lambda^4\phi_h^2}{12} - (m\pi)^2 - \frac{\nu_3}{\phi_h^2}]$$

$$b_{m5} = \phi^2[\frac{\lambda^4\phi_h^2}{12} - \nu_1(m\pi)^2 - \frac{\nu_3}{\phi_h^2}]$$

We now seek solutions for the functions $X_m(\eta)$, $Y_m(\eta)$ and $Z_m(\eta)$, for $m \geq 1$. Introducing the symbol D to indicate differentiation with respect to η we find that the three equations of matrix equations (3.5) can be written as

$$(D^2+b_{m1})X_m(\eta) + b_{m2}Y_m(\eta) + a_{m1}DZ_m(\eta) = 0 \qquad (3.8)$$

$$b_{m3}X_m(\eta) + (D^2+b_{m4})Y_m(\eta) + a_{m2}DZ_m(\eta) = 0 \qquad (3.9)$$

$$b_{m3}DX_m(\eta) + a_{m4}DY_m(\eta) + (D^2+b_{m5})Z_m(\eta) = 0 \qquad (3.10)$$

Operating on these equations with judiciously selected operators, and combining equations (3.8) and (3.9), and then (3.8) and (3.10), we can easily arrive at a pair of equations from which the quantity $Z_m(\eta)$ is eliminated. These two equations are

$$[a_{m2}(D^2+b_{m1}) - a_{m1}b_{m3}]X_m(\eta) + [a_{m2}b_{m1} - a_{m1}(D^2+b_{m4})]Y_m(\eta) = 0 \qquad (3.11)$$

and

$$[(D^2+b_{m5})(D^2+b_{m1}) - a_{m1}a_{m3}D^2]X_m(\eta) + [b_{m2}(D^2+b_{m5}) - a_{m1}a_{m4}D^2]Y_m(\eta) = 0 \qquad (3.12)$$

We are now in a position to combine equations (3.11) and (3.12) in order to obtain an ordinary differential equation involving one of the dependent variables, only. It has been found to be highly desirable, from a computational point of view, to eliminate the variable $X_m(\eta)$. The reasons for the gains experienced in computational efficiency will be addressed shortly.

It is found that after eliminating the variable $X_m(\eta)$ the ordinary differential equation governing the variable $Y_m(\eta)$ may be written as

$$(D^6 + \alpha_{11}D^4 + \alpha_{22}D^2 + \alpha_{33})Y_m(\eta) = 0 \qquad (3.13)$$

where

$$\alpha_{11} = -(\alpha_3 - \alpha_1\alpha_4 - \alpha_6\alpha_7)/\alpha_4$$

$$\alpha_{22} = -(\alpha_3\alpha_1 - \alpha_4\alpha_2 - \alpha_9)/\alpha_4 \qquad (3.14)$$

$$\alpha_{33} = -(\alpha_3\alpha_2 - \alpha_5\alpha_8)/\alpha_4$$

and

$$\alpha_1 = b_{m1} + b_{m5} - a_{m1}a_{m3}\,; \qquad \alpha_2 = b_{m1}b_{m5}\,;$$

$$\alpha_3 = a_{m2}b_{m2} - a_{m1}b_{m4}\,; \qquad \alpha_4 = a_{m1}\,;$$

$$\alpha_5 = a_{m2}b_{m1} - a_{m1}b_{m3}\,; \qquad \alpha_6 = a_{m2}\,; \qquad (3.15)$$

$$\alpha_7 = b_{m2} - a_{m1}a_{m4}\,; \qquad \alpha_8 = b_{m2}b_{m5}\,;$$

$$\alpha_9 = \alpha_6\alpha_8 + \alpha_5\alpha_7\,;$$

We look on the characteristic equation related to equation (3.13) as a cubic equation with associated roots R_1 , R_2 and R_3 . For isotropic materials, theoretical discussions put forth by Cleghorn and Yu [13], indicate these roots will always be real although they may be positive or negative. One of these roots is obtained through a numerical search. Denoting the first root as R_1 , the other two roots become

$$R_2 = -(\alpha_{11} + R_1 - XX)/2 \qquad (3.16)$$

and

$$R_3 = -(\alpha_{11} + R_1 + XX)/2 \qquad (3.17)$$

where

$$XX = (\alpha_{11} + R_1)^2 + 4\alpha_{33}/R_1 \qquad (3.18)$$

Now, redesignating the roots R_1 , R_2 and R_3 if necessary, so that $R_1 > R_2 > R_3$, we

introduce α ,β and γ associated with each value of m, where

$$\alpha = \sqrt{|R_1|} \quad ; \quad \beta = \sqrt{|R_2|} \quad ; \quad \gamma = \sqrt{|R_3|} \tag{3.19}$$

It will be appreciated that associated with negative values of R_1 , R_2 , etc. , there will be a pair of solutions involving trigonometric functions. Conversely, associated with positive values, there will be a pair of hyperbolic functions. It is found expedient at this time to introduce a case number which decides which path the computations are to follow. The parameter "case" is assigned values as follows

$$\begin{aligned} &\text{case} = 1, \quad R_1 \text{ , } R_2 \text{ and } R_3 < 0 \\ &\text{case} = 2, \quad R_1 \text{ and } R_2 < 0 \text{ ; } R_3 > 0 \\ &\text{case} = 3, \quad R_1 < 0 \text{ , } R_2 \text{ and } R_3 > 0 \\ &\text{case} = 4, \quad R_1 \text{ , } R_2 \text{ and } R_3 > 0 \end{aligned} \tag{3.20}$$

It will be apparent from the prescribed boundary conditions , at the edge $\eta = 0$, that the functions $X_m(\eta)$ and $Y_m(\eta)$ must be symmetric with respect to the ξ-axis. Similar reasoning allows us to conclude that the functions $Z_m(\eta)$ must be antisymmetric with respect to the same axis. This means that $X_m(\eta)$ and $Y_m(\eta)$ are even functions of η, and $Z_m(\eta)$ is an odd function of η. We are thus able to eliminate three of the six constants associated with each function. For illustrative purposes, we consider the solution when, case=1. We then have

$$Y_m(\eta) = A_m \cos \alpha\eta + B_m \cos \beta\eta + C_m \cos \gamma\eta \tag{3.21}$$

Of course, had the case been equal to two, the last term of equation (3.21) would have involved cosh $\gamma\eta$. It is not difficult to write solutions associated with other case numbers.

Because of the coupling of the three differential equations, solutions similar in form to equation (3.21) can be written for the functions $X_m(\eta)$ and $Z_m(\eta)$. For the situation, case=1, they take the form

$$X_m(\eta) = A_m R_{m1}\cos\ \alpha\eta + B_m R_{m2}\cos\ \beta\eta + C_m R_{m3}\cos\ \gamma\eta \qquad (3.22)$$

and

$$Z_m(\eta) = A_m S_{m1}\cos\ \alpha\eta + B_m S_{m2}\cos\ \beta\eta + C_m S_{m3}\cos\ \gamma\eta \qquad (3.23)$$

Similar forms of these equations exist for the other case numbers. It is now necessary to develop expressions for the quantities R_{m1} ,S_{m1} , etc. .

Consider the first terms of equations (3.21) and (3.22). Substituting them into equation (3.11) and performing differentiation indicated, it is easily shown that,

$$R_{m1} = \frac{a_{m1}(b_{m4}-\alpha^2) - a_{m2}b_{m2}}{a_{m2}(b_{m1}-\alpha^2) - a_{m1}b_{m3}} \qquad (3.24)$$

Identical expressions are obtained for R_{m2} and R_{m3} of equation (3.22), where α is replaced by β and γ , respectively. Expressions for R_{m1} , R_{m2} , etc. , for the other case numbers are obtained in an identical fashion.

The functions $Y_m(\eta)$ and $Z_m(\eta)$ may be uniquely related by combining equations (3.8) and (3.10) and eliminating the function $X_m(\eta)$. We then obtain

$$[\, a_{m3}b_{m2} - a_{m4}(D^2 + b_{m1})\,]\, DY_m(\eta)$$
$$- [\, D^4 - (a_{m3}a_{m1} - b_{m1} - b_{m5})\, D^2 + b_{m1}b_{m5}]\, Z_m(\eta) = 0 \qquad (3.25)$$

Focusing now on the first term of equations (3.22) and (3.23), and substituting them into equation (3.25), we obtain

$$S_{m1} = \frac{-[\, a_{m4}\alpha^2 - (a_{m4}b_{m1} - a_{m3}b_{m2})\,]\,\alpha}{\alpha^4 + \alpha^2(a_{m3}a_{m1} - b_{m1} - b_{m5}) + b_{m1}b_{m5}} \qquad (3.26)$$

Other expressions for S_{m1} , S_{m2} , etc. , for the various cases can be obtained in an identical fashion.

At this stage, it is appropriate to comment on the decision to solve initially for the function $Y_m(\eta)$ and then express the functions $X_m(\eta)$ and $Z_m(\eta)$ as given in equations (3.22) and (3.23). In fact, in initial computations, a solution was first obtained for the functions $X_m(\eta)$ and expressions similar to those of equations (3.22) and (3.23) were utilized to represent the other two functions. It was found that following such a procedure, the quantities R_{m1} , S_{m1} , etc. , took on values ranging from about ten to the twelfth to ten to the fifteenth power. These massive quantities were generally arrived at through appearance in their denominators of the summation of a pair of equally massive quantities of different signs. This tends to make the computations

unstable as the denominators hovered around zero. Recognizing that the quantities $Y_m(\eta)$ and $Z_m(\eta)$ differed, in general, by only two or three orders of magnitude, it was decided to use the quantity $Y_m(\eta)$ as the reference, as has been done here. The parameters R_{ml} , S_{ml} , etc. , as expected, were found to be extremely small and the summations of massive quantities of almost equal magnitude, but opposite sign appeared in the numerators. This, as expected, has led to a vast improvement in the stability of the computations and the procedure as described here will be followed in future explorations.

Finally, in order to solve for the response of the building block in terms of the Fourier driving coefficients, with $m \geq 1$, it is necessary to establish values for the coefficients A_m ,B_m, etc. , of the above equations. Focusing attention on the edge , η =1, of the first building block we require that the twisting moment $M_{\xi\eta}$ and the transverse shear force Q_ξ should vanish. This is in keeping with Mindlin plate boundary conditions as discussed by Dawe and Roufaeil [21]. Utilizing the expressions provided for twisting moment and transverse shear, equations (2.17), and considering for illustrative purpose the solution when case=1, it is easily shown that we may write

$$Y_m(\eta) = A_m(\cos\ \alpha\eta + X1\cos\ \beta\eta + X2\cos\ \gamma\eta) \qquad (3.27)$$

where X1 and X2 are established through enforcement of the above two boundary conditions.

Next, enforcing the condition of matching of the imposed edge rotation , equation (3.1) and the parameter ψ_η , equation (3.4), along the driven edge, we obtain

$$E_m = A_m(S_{m1}\sin\ \alpha_m + X1\, S_{m2}\sin\ \beta_m + X2\, S_{m3}\sin\ \gamma_m) \qquad (3.28)$$

Denoting the quantity within braces on the right hand side of equation (3.28) as X3, we obtain

$$Y_m(\eta) = \frac{E_m}{X3}(\cos\ \alpha_m\eta + X1\cos\ \beta_m\eta + X2\cos\ \gamma_m\eta) \qquad (3.29)$$

and for $X_m(\eta)$ we have

$$X_m(\eta) = \frac{E_m}{X3}(R_{m1}\cos\ \alpha_m\eta + X1\, R_{m2}\cos\ \beta_m\eta + X2\, R_{m3}\cos\ \gamma_m\eta) \qquad (3.30)$$

with a corresponding expression for $Z_m(\eta)$. There is no difficulty in developing similar expressions for solutions with case=2,3, or 4.

We thus have available an analytical solution for the first building block driven by a harmonic distributed edge rotation where the Fourier subscript m is equal or greater than one. Before generating the eigenvalue matrix, we must examine the case of m = 0, which is a simpler problem where the first building block is driven by a single uniformly distributed harmonic edge rotation.

This is essentially a strip problem. The response of the first building block to this uniform

harmonic edge rotation will be a function of the dimensionless space variable η . Only two equilibrium differential equations are applicable and are written as

$$\frac{\partial^2 W}{\partial \eta^2} + \phi \frac{\partial^2 \psi_\eta}{\partial \eta^2} + \frac{\lambda^4 \phi^2 \phi_h^2 W}{\nu_3} = 0 \tag{3.31}$$

$$\frac{\partial^2 \psi_\eta}{\partial \eta^2} - \frac{\nu_3 \phi^2}{\phi_h^2} \left(\psi_\eta + \frac{1}{\phi} \frac{\partial W}{\partial \eta} \right) + \frac{\lambda^4 \phi^2 \phi_h^2 \psi_\eta}{12} = 0 \tag{3.32}$$

The dependent variables W and ψ_η , both functions of η are written as

$$W(\eta) = X(\eta) \tag{3.33}$$

and

$$\psi_\eta(\eta) = Z(\eta) \tag{3.34}$$

We therefore have, following earlier nomenclature and substituting in equations (3.31) and (3.32)

$$X''(\eta) + a_{m1} Z'(\eta) + b_{m1} X(\eta) = 0 \tag{3.35}$$

and

$$Z''(\eta) + a_{m3} X'(\eta) + b_{m5} Z(\eta) = 0 \tag{3.36}$$

which are the one dimensional counterpart of equations (3.5) and where

$$a_{m1} = \phi$$

$$a_{m2} = -\nu_3\phi/\phi_h^2$$
$$b_{m1} = \lambda^4\phi^2\phi_h^2/\nu_3 \qquad (3.37)$$
$$b_{m5} = \lambda^4\phi^2\phi_h^2/12 - \nu_3\phi^2/\phi_h^2$$

Again, introducing the differential operator D, we have

$$(D^2+b_{m1})X(\eta) + a_{m1}DZ(\eta) = 0 \qquad (3.38)$$

and

$$a_{m3}DX(\eta) + (D^2+b_{m5})Z(\eta) = 0 \qquad (3.39)$$

For this first term of the building block representation, we choose to eliminate the quantity $Z(\eta)$ from equations (3.38) and (3.39), and we obtain

$$(D^4 + \alpha_{11}D^2 + \alpha_{22})X(\eta) = 0 \qquad (3.40)$$

where

$$\alpha_{11} = b_{m5} + b_{m1} - a_{m1}a_{m3}$$
$$\alpha_{22} = b_{m5}b_{m1} \qquad (3.40a)$$

The characteristic equation associated with equation (3.40) may be considered as a quadratic equation with roots R_1 and R_2 .

We now have three possible cases as follows

$$\begin{aligned} &\text{case} = 1, \quad && R_1 \text{ and } R_2 < 0 \\ &\text{case} = 2, \quad && R_1 < 0 \,;\; R_2 > 0 \\ &\text{case} = 3, \quad && R_1 \text{ and } R_2 > 0 \end{aligned} \tag{3.41}$$

Designating the roots in such a way that $R_2 > R_1$, and introducing

$$\alpha = \sqrt{|R_1|} \quad ; \quad \beta = \sqrt{|R_2|} \tag{3.42}$$

we write for case=1

$$X(\eta) = A_m \cos \alpha\eta + B_m \cos \beta\eta \tag{3.43}$$

and

$$Z(\eta) = A_m S_{m1} \cos \alpha\eta + B_m S_{m2} \cos \beta\eta \tag{3.44}$$

with similar expressions involving hyperbolic and trigonometric functions, or hyperbolic functions only for case=2, and case=3, respectively. Again, two of the constants have been eliminated because of boundary conditions along the edge, η =0.

Following steps parallel to those described earlier, we are able to develop expressions for the quantities S_{m1} and S_{m2} for each case. Finally, enforcing boundary conditions imposed along the edge, η =1, we express the functions $X(\eta)$ and $Z(\eta)$ in terms of the harmonic edge rotation E_m (m=0).

We then write, for case=1,

$$X(\eta) = \frac{E_m(m=0)}{X2}(\cos \alpha\eta + X1 \cos \beta\eta) \tag{3.45}$$

and

$$Z(\eta) = \frac{E_m(m=0)}{X2}(S_{m1}\cos \alpha\eta + X1S_{m2}\cos \beta\eta) \tag{3.46}$$

where X1 and X2 depend on the boundary conditions.

Similar expressions are obtained for the other two cases.

The second building block of Figure 1 differs from the first only in that it is driven along the edge, ξ =1. To avoid confusion, we will designate the Fourier driving coefficients for this building block by the symbols E_n . The solution for the response of this building block is available from that of the first provided we take the following steps

a) replace λ^2 by $\lambda^2\phi^2$,

b) replace ϕ_h by ϕ_h/ϕ ,

c) replace ϕ by $1/\phi$,

d) replace the symbol m by n.

The lateral displacement for the second building block will take the form

$$W(\xi, \eta) = \sum_{n=0,1}^{\infty} X_n(\xi) \cos n\pi\eta \tag{3.47}$$

The third and fourth building blocks are also driven by distributed harmonic edge rotations. We use the subscripts p and q, respectively, for the Fourier driving coefficient subscripts. Beyond this, the third building block solution differs from the first only in that the η of the first building block must be replaced by $1-\eta$. Similarly, the fourth building block solution is extracted from that of the second building block through replacing ξ with $1-\xi$.

We are now ready to construct the eigenvalue matrix. Such a matrix, based on a three term solution for the building blocks, is shown schematically in Figure 2.

The matrix is developed in a manner identical to that followed for thin plates, Gorman [3]. Small inset figures at the top of the main figure indicate the building blocks pertinent to the column below. Other small insets to the right of the figure indicate the boundary conditions to be satisfied.

It will be recognized that the net bending moment along the edge, $\eta=1$, of the superimposed set of building blocks must be equal to zero. Toward this end, the contributions of each building block to moment along this edge are expanded in a cosine series. Each term in this series is set equal to zero. This gives rise to a set of K+1 homogenous algebraic equations relating the Fourier driving coefficients. K equals the upper limit of subscripts in the Fourier expressions. Similar equations are obtained for the other three edges. We thus arrive at a set of 4K+4 equations relating the 4K+4 Fourier unknown driving coefficients. The coefficient matrix of this set of equations forms our eigenvalue matrix. Eigenvalues for the problem are equal to

those values of the parameter λ^2 which cause the determinant of the matrix to vanish.

It is worth noting that with the aid of physical reasoning, much of the work normally required in generating the eigenvalue matrix can be avoided. This leads to a reduction in the possibility of error. It will be noted that there is a 4 by 4 array of segments in the matrix, Figure 2. Let us suppose we have computed the four segments immediately underneath the first building block. An identical computer algorithm can be used to generate the four segments immediately beneath the second building block provided we make the changes (a) to (d) as itemized earlier for generation of this second building block. Of course, the matrix element subscripts will have to be adjusted as required.

There is no need to generate the matrix segment immediately beneath the third and fourth building block. They can be transferred from segments beneath the first two building block, with sign modifications as required. Let us denote the segments by the subscripts (i,j). It is found that the following pairs of matrix segments are identical,

segment (1,1) = segment (3,3)

segment (3,1) = segment (1,3)

segment (4,4) = segment (2,2)

segment (2,4) = segment (4,2)

The following segments beneath the third and fourth building blocks may be transferred from corresponding segment of the first two building blocks provided a sign change is introduced

in the second, fourth, sixth rows, etc. , as the transfer is made.

segment (2,3) is obtained from segment (2,1)

segment (4,3) is obtained from segment (4,1)

segment (1,4) is obtained from segment (1,2)

segment (3,4) is obtained from segment (3,2)

Similar, but not identical, matrix segment transfer rules apply when all plate edges are clamped.

3.1.2 Presentation of Computed Results

Eigenvalues were computed for the first ten modes of flexural vibration with value of the parameter ϕ_h equal to 0.01, 0.02, 0.04, 0.06, 0.08 and 0.10 . Plate aspect ratios employed were 1.0, 1.25, 1.5, 2.0, 2.5, and 3.0 . Due to symmetry, it was not necessary to investigate behaviour of plates with aspect ratio less than 1 . For low values of thickness parameter one expects the computed eigenvalues to be in close accord with those computed by the thin plate theory, Gorman [4] . In fact, this latter set of eigenvalues provided jumping-off points for Mindlin plate study.

Computed eigenvalues are tabulated in Table A.1 and A.6 , a different plate aspect ratio is associated with each table. It will also be noted that one column, designated by the symbol, TPT (thin-plate theory), is provided in each table. Taken from Gorman [4], this column provides limits which the computed results are expected to closely approach as the parameter ϕ_h is allowed to approach zero. One must recall, however, that the T.P.T. results were computed

without inclusion of rotary inertia effects. Furthermore, the Mindlin plate theory may be considered as slightly more restrictive, as a condition of zero twisting moment and zero transverse shear is enforced along the plate edges. In the thin-plate theory, of course, only the condition of zero vertical edge reaction, as developed by Kirchhoff, is enforced. A value of the parameter κ^2 equal to 0.8601 was employed in all computations. This is the same value as utilized by Dawe & Roufaeil [21], in their fully clamped plate calculations. They used slightly different values in some of their other calculations in order to facilitate comparison of their results with that of some of their predecessors. There are two very close commonly used values, 5/6 and $\pi^2/12$, which were first introduced by Reissner [1] and Mindlin [2],respectively. However in tests conducted during the present research, it was found that a limited range of variation in the assumed values of κ^2 had no significant effect on the computed eigenvalues.

The character of the mode shapes associated with each thin-plate-theory eigenvalue is indicated in each table under the heading "Type". Modes symmetric and antisymmetric, about plate central axis, running parallel to the ξ and η directions are indicated by the symbol "SYM" and "ASYM", respectively. The symbol "S-A" indicates modes symmetric about the central axis running in the ξ-direction and antisymmetric about the other central axis. The symbol "A-S" has just the opposite significance. All symmetric-antisymmetric modes of the square plate , Table A.1, will have double roots, or double eigenvalues, associated with them. For illustrate purposes, the first three mode shapes of the square plate are presented in Figure A.1 through A.3 .

All data presented has been computed utilizing 7-term expansions for the plate lateral

displacement and slope functions. It was found that utilization of more terms did not affect the fourth digit in the computed eigenvalues. A study of these tables indicates that for each mode the eigenvalue approaches extremely close to that of thin-plate-theory as the parameter ϕ_h decreases. For ϕ_h = 0.01, it is found in most cases that any difference between the computed eigenvalues and the thin-plate-theory eigenvalues involves the fourth digit only. This is in keeping with experience of Cleghorn and Yu [13], for example.

It will be noted that, in general, the rate of decrease in computed eigenvalue with increase in the parameter ϕ_h is much greater for the higher modes. It is generally agreed that even the Mindlin theory will not be reliable if one applies it to very high mode studies. This is because the ratio of plate thickness to inter-node distances will become too large. Even though the present calculations have been utilized to study up to 10 modes, it will be recognized that because of the various mode families involved, the ratio of plate thickness to inter-node distance is still reasonable.

3.2 Completely Free Symmetric Cross-ply Plates

3.2.1 Mathematical Procedure

The governing differential equations for symmetric cross-ply plates are those developed in chapter 2, equation (2.24). The same four building blocks, edge driven forced vibration problems, as presented schematically in Figure 1, are employed here to obtain the solution to the

free vibration problem of completely free symmetric cross-ply plates.

Only the obtaining of a solution for the first building block needs to be described in detail. The three non-driven edges of this building block are still given slip shear support. The driven edge of the first building block is free of transverse shear stress and twisting moment. It is subjected to a distributed harmonic edge rotation with amplitude given as equation (3.1). The Levy type solutions which are used for completely free isotropic thick plate, equations (3.2) to (3.4) can still be used here as solutions for the first building block. Substituting these Levy type solutions into governing differential equations (2.24), we obtain a set of three simultaneous coupled ordinary differential equations which are represented in same matrix form as equations (3.5), but the values of the matrix element a_{ml} , b_{ml} , etc. are different from those of equations (3.6) and (3.7). They take on the following expressions

$$
\begin{aligned}
a_{m1} &= \phi \\
a_{m2} &= -(d_{12}+d_{66})\, m\pi\phi / d_{66} \\
a_{m3} &= -\kappa^2 a_{44}\phi / \phi_h^2 d_{22} \\
a_{m4} &= (d_{12}+d_{66})\, m\pi\phi / d_{66}
\end{aligned}
\qquad (3.48)
$$

and

$$
b_{m1} = \frac{\lambda^4\phi_h^2 - (m\pi)^2\kappa^2 a_{55}}{\kappa^2 a_{44}}\phi^2
$$

$$
b_{m2} = \frac{a_{55}(m\pi)}{a_{44}}\phi^2
$$

$$b_{m3} = \frac{\kappa^2 a_{55}(m\pi)}{\phi_h^2 d_{66}}\phi^2 \tag{3.49}$$

$$b_{m4} = \frac{\lambda^4\phi_h^2 - d_{11}(m\pi)^2 - \kappa^2 a_{55}/\phi_h^2}{d_{66}}\phi^2$$

$$b_{m5} = \frac{\lambda^4\phi_h^2 - d_{66}(m\pi)^2 - \kappa^2 a_{44}/\phi_h^2}{d_{22}}\phi^2$$

Following the same procedures as we did before, we finally get a sixth order ordinary homogeneous differential equation involving the function $Y_m(\eta)$ after eliminating the functions $X_m(\eta)$ and $Z_m(\eta)$. The characteristic equation related to this equation is written as

$$\varepsilon^6 + \alpha_{11}\varepsilon^4 + \alpha_{22}\varepsilon^2 + \alpha_{33} = 0 \tag{3.50}$$

where α_{11} , α_{22} etc. have the same expressions as defined in equations (3.14) and (3.15).

This is a cubic equation in the quantity ε^2 . For ε^2 there will be one real root, positive or negative, which must be found by a numerical search. With this root found, the characteristic equation is reduced to a quadratic equation. For composite materials, the two remaining roots could be a real or a complex conjugate pair. Associated with each of the three roots for ε^2 , there will be a further pair of roots, each pair providing terms contributing toward the formulation of the function $Y_m(\eta)$. We will see that the complex roots constitute more complicated

expressions.

It is not advisable here to try and discuss all possible combinations of roots and the associated form of the solution for $Y_m(\eta)$. Let us assume, for illustrative purpose, that all three roots for the quantity ε^2 are real and negative. Denote the magnitude of these roots as ε_1^2 ,ε_2^2 and ε_3^2 . The same reasoning from the prescribed boundary conditions at the edge η =0, as we did before, allows us to conclude that the functions $X_m(\eta)$ and $Y_m(\eta)$ must be symmetric with respect to the ξ-axis, and the function $Z_m(\eta)$ must be anti-symmetric with respect to the same axis. Thus we can write function $Y_m(\eta)$ as

$$Y_m(\eta) = A_m \cos \varepsilon_1 \eta + B_m \cos \varepsilon_2 \eta + C_m \cos \varepsilon_3 \eta \qquad (3.52)$$

Similarly, if all the roots for the quantity ε^2 were real and positive, the trigonometric functions, sine and cosine of equation (3.52), would have to be replaced respectively by hyperbolic sine and hyperbolic cosine functions. Up to now, the expressions for $Y_m(\eta)$ are similar to those in previous isotropic thick plate case.

We now illustrate the solution for $Y_m(\eta)$ in the situation where a pair of complex roots for the ε^2 are obtained. Let us suppose we have a pair of complex conjugate roots where $\varepsilon_2^2 = a + bi$ and $\varepsilon_3^2 = a - bi$. We introduce $X = \sqrt{a^2 + b^2}$, and $Y = \tan^{-1}(b/a)$, next, introduce R = X sin(Y/2), and S = X cos(Y/2). Assuming ε_1^2 is negative, dropping terms anti-symmetric with respect to ξ-axis, we obtain for $Y_m(\eta)$

$$Y_m(\eta) = A_m \cos \varepsilon_1 \eta + B_m \cos R\eta \cosh S\eta + C_m \sin R\eta \sinh S\eta \qquad (3.53)$$

Having obtained expressions for $Y_m(\eta)$, corresponding expressions for the functions $X_m(\eta)$ and $Z_m(\eta)$ are obtained. For example, with $Y_m(\eta)$ written as equation (3.52), the functions $X_m(\eta)$ and $Z_m(\eta)$ are written as

$$X_m(\eta) = A_m R_{m1} \cos \varepsilon_1 \eta + B_m R_{m2} \cos \varepsilon_2 \eta + C_m R_{m3} \cos \varepsilon_3 \eta \qquad (3.54)$$

and

$$Z_m(\eta) = A_m S_{m1} \sin \varepsilon_1 \eta + B_m S_{m2} \sin \varepsilon_2 \eta + C_m S_{m3} \sin \varepsilon_3 \eta \qquad (3.55)$$

where the quantities R_{m1} , S_{m1} , etc. are obtained through manipulation of equations (3.5). With $Y_m(\eta)$ written as equation (3.53), the functions $X_m(\eta)$ and $Z_m(\eta)$ are written as

$$\begin{aligned} X_m(\eta) = {} & A_m R_{m1} \cos \varepsilon_1 \eta + (R_{m2} B_m + R_{m3} C_m) \cos R\eta \cosh S\eta \\ & + (-R_{m3} B_m + R_{m2} C_m) \sin R\eta \sinh S\eta \end{aligned} \qquad (3.56)$$

and

$$\begin{aligned} Z_m(\eta) = {} & A_m R_{m1} \sin \varepsilon_1 \eta + (S_{m2} B_m + S_{m3} C_m) \cos R\eta \sinh S\eta \\ & + (S_{m3} B_m - S_{m2} C_m) \sin R\eta \cosh S\eta \end{aligned} \qquad (3.57)$$

where the quantities R_{m1} , S_{m1} , etc. can also be obtained through manipulation of equations (3.5).

With provision made in the analysis for all possible combinations of roots of the characteristic equation (3.50) and associated solutions, we must turn to evaluation of the boundary conditions along the edge, $\eta = 1$. Again we must enforce the conditions of zero twisting moment, zero transverse shear force, and matching of imposed edge rotation and the parameter ψ_η, at the edge $\eta=1$. Referring to equations (2.26), (3.1), (3.2), (3.3) and (3.4), it is seen that the boundary conditions are formulated respectively as

$$\frac{1}{\phi}\frac{\partial Y_m(\eta)}{\partial \eta} - m\pi Z_m(\eta) = 0$$

$$Z_m(\eta) + \frac{1}{\phi}\frac{\partial X_m(\eta)}{\partial \eta} = 0 \qquad (3.58)$$

$$\psi_\eta = E_m$$

Enforcing these boundary conditions for each solution form of interest, we establish the coefficients A_m, B_m and C_m, as discussed earlier. We now have the exact forced vibration response available for the first building block, for any distributed harmonic edge rotation as represented in equation (3.1) with subscript m greater than zero.

We turn now briefly to the situation when the above subscript m takes on the value zero. Examining the first building block of Figure 1, it is seen that under this condition the driven edge is subjected to a uniform rotation and the response of the building block will coincide with that of a beam or strip. This means that the slope function ψ_ξ will be everywhere zero. Furthermore,

all derivatives with respect to the coordinate ξ will also equal zero. Displacement W and rotation ψ_η will be functions of η only. From equations (3.2) and (3.4), again we write the solutions for W and ψ_η in the same form as equations (3.33) and (3.34).

Returning to the equilibrium equations, we see that only first and third equations of equation (2.24) are applicable. Deleting terms involving derivatives with respect to the coordinate ξ , and substituting from equations (3.33) and (3.34) as before, we obtain the pair of coupled ordinary differential equations which have the same expressions as equations (3.35) and (3.36). However, the quantities a_{ml} , b_{ml} , etc. differ from those of equations (3.37). They have the similar form to those of equations (3.48) and (3.49), the only difference lies in that components involving the mm must be dropped. Again, primes imply differentiation with respect to η .

Equations (3.35) and (3.36) are solved in a similar manner identical to that described earlier for the set of equations (3.5). In the work undertaken here, it was decided to eliminate the function $Z(\eta)$ by manipulation of equations (3.35) and (3.36). The resulting differential equation is therefore quadratic in the parameter ε^2 as discussed earlier. The roots of the characteristic equation may therefore be written immediately. Expressions for $X(\eta)$ and $Z(\eta)$ will contain only two unknowns after enforcement of the required symmetry or antisymmetry about the origin. These two unknowns are evaluated through enforcement of conditions of zero lateral shear force and matching of edge rotations at the edge, η =1. This completes computation of response of the first building block to the harmonic rotation distributed along its driven edge.

It is obvious that a solution for the second building block of Figure 1 can be obtained by following steps identical to those described above for the first building block, provided appropriate changes in the input parameters are introduced. In fact, the second building block constitutes a mirror image of the first one. These changes in the input parameters will be discussed shortly. It is also apparent that solutions for the third and fourth building blocks can be extracted from those of the first and second by simply replacing the variables ξ and η with $(1-\xi)$ and $(1-\eta)$, respectively.

With solutions for the four building blocks available, the eigenvalue matrix is generated following established procedures. First, the four building block solutions are superimposed one upon the other. Then, the net bending moment along each edge is expanded in a series of K terms where K is also the number of terms used in the building block solution series.

It is found advantageous to use the same cosine series as used in the individual solutions to represent the net bending moment expansions. Each net coefficient in the four bending moment expansions is set equal to zero. This gives rise to a set of 4K+1 simultaneous homogenous algebraic equations relating the 4K+1 unknown Fourier driven coefficients. The coefficient matrix of this set of equations becomes the eigenvalue matrix. Eigenvalues are those values of the parameter λ^2 which cause the determinant of the eigenvalue matrix to vanish. With eigenvalues established the associated mode shapes are obtained by setting one of the non-zero driving coefficients equal to unity and solving for the other coefficients. Mode shapes can then be plotted.

3.2.2 Presentation of Computed Results

The illustrative cross-ply problem utilized is that described by Khdeir [19]. The laminated plate consists of three identical orthotropic laminae in a $(0^0/\ 90^0/\ 0^0)$ configuration. Utilizing conventional notation, the orthotropic properties are given as

$$E_1/E_2 = 40\ ,\ G_{12}/E_2 = G_{13}/E_2 = 0.6\ ,\ G_{23}/E_2 = 0.5 \quad \text{and} \quad \nu_{12} = 0.25$$

From equations (2.19), (2.21) and (2.25), we have

$$a_{44} = \frac{2}{3}(G_{23}/E_2 + 0.5G_{13}/E_2)$$

$$a_{55} = \frac{2}{3}(0.5G_{23}/E_2 + G_{13}/E_2)$$

$$d_{11} = (E_1/E_2 + 0.0385)/1.0385\,XX$$

$$d_{12} = \nu_{12}/XX$$

$$d_{22} = (1 + 0.0385\,E_1/E_2)/1.0385\,XX$$

$$d_{66} = G_{12}/12E_2$$

where $XX = 12(1 - \nu_{12}\nu_{21})$

Before presenting the computed data, it is appropriate to point out certain simplifications which have been utilized in computations related to the present work.

The schematic representation of the eigenvalue matrix is the same presented in Figure 2. It will be appreciated that with the solution for the first building block available, all of the elements of the four matrix segments immediately below this building block are entered.

The same computer routine utilized to generate the above elements may also be utilized to generate the elements of the matrix components immediately below the second building block in Figure 2. It is only necessary to make the following modifications to the input parameters.

a) replace λ^2 with $\lambda^2\phi^2\sqrt{E_1/E_2}$

replace ϕ_h with ϕ_h/ϕ

replace ϕ with $1/\phi$

b) set $E_1/E_2 = 1/40$, $G_{12}/E_2 = G_{13}/E_2 = 0.6/40$, $G_{23}/E_2 = 0.5/40$

and $\nu_{12} = 0.25/40$

The solution for the second building block lateral displacement will now take the form as equation (3.47).

Finally, physical reasoning tells us that elements required for completing the matrix segments beneath the third and fourth building blocks of Figure 2 can be transferred with appropriate sign changes, in the same way described earlier in the thick isotropic plate case, from those beneath the first and second building blocks.

Before generating eigenvalues for problems of interest, it is necessary to select a value for K, the number of terms in the solution series expansions, and κ^2 , the shear correction factor.

After conducting a sequence of convergence studies, it was decided to adopt a value of K=7. Experience indicated that increasing this number would not change the fourth significant digit in computed eigenvalues. Following the practice of Yu et al [15], a value of 0.8601 was adopted for the parameter κ^2 . It was found that eigenvalues were not very sensitive to small changes in this parameter.

Because in the authors experience there appears to be no published results pertaining to the completely free cross-ply problem of interest, it was decided to run verification tests on the present analysis by comparing computed results with those obtained by Gorman [6] in a study of completely free thin orthotropic plates. In this earlier study, attention was focused on the family of problems where flexural rigidities were considered to satisfy the condition $\sqrt{D_x D_y}$, where D_x and D_y are flexural rigidities associated with the x, (ξ) and y, (η) directions respectively, and H is the plate torsional rigidity. It was decided to compare results obtained by the present analysis with those of the earlier one for the situation where $D_x / D_y = 4.0$. Since the thin plate analysis essentially assumes that the parameters G_{13} and G_{23} are equal to infinity, large values (three times G_{12}) were given to them when employing the present analysis. Of course the earlier orthotropic problem corresponds to the present problem where we have only one ply in the assemblage.

In Table A.7, eigenvalues computed by the present method are compared with those reported in reference [6] for a thin plate with $D_x / D_y = 4.0$ and $H = \sqrt{D_x D_y}$. Results are compared for six modes and various plate aspect ratios.

It is seen that there is very good agreement between the two sets of results. Where there are slight differences (usually involving the fourth significant digit only) the results of the present study are seen to be slightly lower. This is to be expected since the earlier thin plate analysis neglects effects of rotary inertia and assumes zero transverse shear induced deformation. Both of these factors lead to the prediction of slightly higher eigenvalues. We can conclude therefore that the results of Table A.7 constitute strong evidence supporting the validity of the present analysis.

In Table A.8, computed eigenvalues are presented for the 0/90/0 laminated cross-ply plate as used for illustrative purposes by Khdeir but with completely free edges. For a thickness-to-length ratio, h/a = 0.1, and results are tabulated for the first four modes with aspect ratio varying between 1.0 and 2.0 . Further results are presented in Table A.9 where the inverse of the aspect ratio varies between 1.0 and 2.0 . There is unfortunately no known published results against which the present data can be compared.

The associated first three mode shapes of the symmetric cross-ply square plate are presented in Figure A.4 through A.6 .

Chapter 4

The Superposition-Galerkin Method for Analyzing Rectangular Plates With Combinations of Clamped and Simply Supported Edge Conditions

As we have already seen in chapter 3, the exploitation of the traditional superposition method for analyzing free vibration problems becomes a more and more demanding and complicated task when one moves away from the thin isotropic theory to the thick plate Mindlin theory, and to analysis of laminated plates. Difficulties arise because of the vast families of roots encountered, real and complex, when solving associated differential equations. The presence of hyperbolic functions tends to produce computer over-flow and under-flow and even computational instability problems.

In this chapter, the modified "Superposition-Galerkin" method is introduced as a much more viable means for resolving the problems of free vibration of symmetric cross-ply laminated plates with any combination of clamped and simply supported boundary conditions. It is shown

how this new approach leads to vast simplification in the computational procedure with the same accurate eigenvalues being obtained.

4.1 Mathematical Procedure

The governing differential equations for clamped and simply supported laminated plates are still those developed in chapter 2, equations (2.24). A solution to the free vibration of a fully clamped symmetric cross-ply laminated plates is achieved by superimposing individual solutions to the four forced vibration problems (building block), represented schematically in Figure 3. Following superposition, Fourier driving coefficients appearing in the problem are so constrained as to fulfil the condition of zero net slope along all four edges of the plate.

We now focus attention on the first building block for which the forced vibration will now be obtained by the Galerkin technique. This building block, which has simple support along all non-driven edges, is driven by a harmonic bending moment with amplitude distribution

$$M_\eta = \sum_{m=1}^{\infty} E_m \sin\ m\pi\xi \tag{4.1}$$

The solution is written in the form proposed by Levy as

$$W(\xi, \eta) = \sum_{m=1}^{\infty} X_m(\eta) \sin\ m\pi\xi \tag{4.2}$$

$$\psi_\xi(\xi, \eta) = \sum_{m=1}^{\infty} Y_m(\eta) \cos m\pi\xi \tag{4.3}$$

$$\psi_\eta(\xi, \eta) = \sum_{m=1}^{\infty} Z_m(\eta) \sin m\pi\xi \tag{4.4}$$

Choosing any arbitrary value of "m" and substituting equations (4.2) to (4.4) into governing differential equations, equations (2.24), we obtain a set of coupled ordinary differential equations which are written in same matrix form as equations (3.5), but the values of the matrix elements are different, they have the following expressions

$$\begin{aligned} a_{m1} &= \phi \\ a_{m2} &= (d_{12} + d_{66})\, m\pi\phi / d_{66} \\ a_{m3} &= -\kappa^2 a_{44}\phi / \phi_h^2 d_{22} \\ a_{m4} &= -(d_{12} + d_{66})\, m\pi\phi / d_{22} \end{aligned} \tag{4.5}$$

and

$$b_{m1} = \frac{\lambda^4 \phi_h^2 - \kappa^2 a_{55} (m\pi)^2}{\kappa^2 a_{44}} \phi$$

$$b_{m2} = \frac{-a_{55} m\pi\phi}{a_{44}}$$

$$b_{m3} = \frac{-\kappa^2 a_{55} m\pi\phi}{\phi_h^2 d_{66}} \tag{4.6}$$

$$b_{m4} = \frac{\lambda^4 \phi_h^2 / 12 - d_{11}(m\pi)^2 - \kappa^2 a_{55} / \phi_h^2}{d_{66}} \phi^2$$

$$b_{m5} = \frac{\lambda^4 \phi_h^2 / 12 - d_{66}(m\pi)^2 - \kappa^2 a_{44} / \phi_h^2}{d_{22}} \phi^2$$

We now expand function $X_m(\eta)$, $Y_m(\eta)$ and $Z_m(\eta)$ into series form. Because we will be employing the Galerkin method, the boundary conditions must be satisfied exactly by each term in these series. The functions $X_m(\eta)$ and $Y_m(\eta)$ must equal zero at each extremity. We therefore write

$$X_m(\eta) = \sum_{i=1,2}^{k} E_i \sin i\pi\eta \tag{4.7}$$

$$Y_m(\eta) = \sum_{j=1,2}^{k} E_j \sin j\pi\eta \tag{4.8}$$

It will be obvious that the function $Z_m(\eta)$ must be symmetrically distributed with respect to the ξ axis. It must also be distributed in such a way that the moment equilibrium condition is satisfied along the edge, η=1 . We achieved these goals by expressing $Z_m(\eta)$ as

$$Z_m(\eta) = \sum_{l=1,2}^{k} E_l \cos (l-1)\pi\eta + E_m \frac{\eta^2}{2} \tag{4.9}$$

With the series for the dependent variables selected, the standard Galerkin procedure is followed. First the series of equations (4.7) to (4.9) are differentiated term by term and

substituted into the governing differential equations (3.5). This provides three quantities which we designate as Q_1 , Q_2 and Q_3 ,

$$Q_1 = \sum_{i=1}^{k} E_i [\, b_{m1} - (i\,\pi)^2] \sin\, i\,\pi\eta + b_{m2} \sum_{j=1}^{k} E_j \sin\, j\,\pi\eta$$

$$- a_{m1} \sum_{l=1}^{k} E_l (l-1)\,\pi \sin\, (l-1)\,\pi\eta + a_{m1} E_m \eta$$

$$Q_2 = b_{m3} \sum_{i=1}^{k} E_i \sin\, i\,\pi\eta + \sum_{j=1}^{k} b_{m2} E_j [\, b_{m4} - (j\,\pi)^2] \sin\, j\,\pi\eta$$

$$- a_{m2} \sum_{l=1}^{k} E_l (l-1)\,\pi \sin\, (l-1)\,\pi\eta + a_{m2} E_m \eta \qquad (4.10)$$

$$Q_3 = a_{m3} \sum_{i=1}^{k} E_i (i\,\pi) \cos\, i\,\pi\eta + a_{m4} \sum_{j=1}^{k} E_j (j\,\pi) \cos\, j\,\pi\eta$$

$$+ \sum_{l=1}^{k} E_l [\, b_{m5} - (l-1)^2 \pi^2] \cos\, (l-1)\,\pi\eta + E_m \left(1 + b_{m5} \frac{\eta^2}{2}\right)$$

Each quantity contains the driving coefficients E_m , the Fourier coefficients E_i , E_j , etc. , and may be thought of as representing the error in the differential equation solutions.

Finally, we expand each of the quantities, Q_1 , Q_2 , etc. , in an appropriate Fourier series and require that each coefficient in these series should vanish. This provides us with 3K simultaneous non-homogeneous algebraic equations relating the above Fourier coefficients. A

solution for these coefficients is obtained immediately and we thus have available the response of the building block to the harmonic driving moment component.

It is found advantageous to expand the functions Q_1 and Q_2 in sine series while Q_3 is expanded in a cosine series. In this way we take advantage of orthogonality of the trigonometric series and the problem of setting up the matrix associated with above set of equations is greatly simplified. A schematic representation of these equations in matrix form is shown in Figure 4 for four-term expansions of the series representing the dependent variables. It will be observed that the main matrix divides naturally into nine segments. Only diagonal, or off-diagonal elements in these segments are non-zero. Furthermore, all integrals required for generating the main matrix will equal one half.

With the coefficient of equations (4.7) to (4.9) established, the response of the first building block is known. It is obvious that with a simple interchange of variables, similar to what we did before in chapter 3, one can achieve the response of the second building block. Responses of the third and fourth building block may be obtained from that of the first and second by replacing the variable ξ and η , with $1 - \xi$ and $1 - \eta$, respectively.

A solution to free vibration problem is achieved following established procedures. The four building blocks are superimposed and their contributions to slope along each edge are expanded in a Fourier series. It is required that the net coefficient in each of these series must vanish. Let us say there are KK terms in the building block expansions. Expanding the

contributions to slope along each edge gives rise to a set of 4KK homogenous algebraic equations relating 4KK unknown Fourier driving coefficients. Eigenvalues of the problem are obtained by requiring the determinant of the coefficient matrix for the above set of equations to vanish.

It is already apparent that the Galerkin modification vastly simplifies the problem of analyzing free vibration of symmetric cross-ply laminated plates by the superposition method. These simplifications will be discussed in detail later.

4.2 Presentation of Computed Results

The illustrative cross-ply problem utilized here is still that described by Khdeir [19]. The materials properties and input parameters are the same presented before in section 3.2.2 .

Before presenting the computed data it is appropriate to point out certain simplifications which have been utilized in computations related to present work.

A schematic representation of the eigenvalue matrix is presented in Figure 5. It is observed that the matrix is made up of 16 segments. four under each building block. Small insert to the right indicate edges along which the net slope, (SL), is constrained to equal zero. It will be appreciated that with the solution for the first building block available all of the elements of the four matrix segments immediately below the first building block are entered. Sine series have been utilized to expanded the net slope along each edge.

The same computer routine utilized to generate the above elements may also be utilized to generate the elements of the matrix components immediately below the second building block in Figure 5. It is only necessary to make the same modifications to the input parameters as we did before in section 3.2.2 .

The solution for the second building block displacement will now take the form

$$W(\xi, \eta) = \sum_{n=1}^{\infty} X_n(\xi) \sin n\pi\eta \qquad (4.11)$$

Finally, physical reasoning tells us that elements required for completing the matrix segments beneath the third and fourth building blocks of Figure 5 can be transferred, with appropriate sign changes, from those of the first and second building blocks.

Let us denote each of the 4 by 4 array of segments making up the eigenvalue matrix of Figure 5 by the letter (i,j), where i indicates the row and j indicate the column. Then we have

segment (3,3) = - segment (1,1)

segment (1,3) = - segment (3,1)

segment (4,4) = - segment (2,2)

segment (2,4) = - segment (4,2)

The remaining segments may be obtained from those on the left hand side of Figure provided a sign change is introduced in every second row of the new segments. We proceed as

follows

obtain segment (2,3) from segment (2,1)

obtain segment (4,3) from segment (4,1)

obtain segment (1,4) from segment (1,2)

obtain segment (3,4) from segment (3,2)

Before computing eigenvalues, it is necessary to decide on the number of terms to be utilized in the series expansions in order to obtain the required convergence. Two limits must be established. They are the number of terms, K, to be utilized in the Galerkin solutions, and the number of terms, KK, to be utilized in the building block driving moment expansions. The eigenvalue matrix will be of size 4KK by 4KK. Experience has shown that values of 22 and 7, for K and KK, respectively, will give four significant digits in the computed eigenvalues. These were the values employed in the Superposition-Galerkin method studies reported here. A value of 0.8601 has been utilized for κ^2 , the shear correction factor, in all computations reported here. The same value was utilized by Yu et al.

While the analysis as described up to this point relates to the fully clamped plate, it will be appreciated that by deleting appropriate building blocks, and corresponding sections of the eigenvalue matrix, plates with any combination of clamped and simply supported boundary conditions can be analyzed. Using the letter C and S to indicate clamped and simply supported edges, respectively, each plate is designated by a sequence of four letters. These letter designations indicate the edge conditions beginning at the edge, ξ =0, and moving anti-clockwise

around the plate.

In Table A.10 eigenvalues computed by various methods are tabulated for SSSC and SCSC square plates, for various values of the ratio E_1/E_2 . The thickness ratio ϕ_h is equal to 0.1 . The symbols HSDPT and HSDT refer to eigenvalues listed by Khdeir [19] and obtained by means of higher order shear deformation theories. It is seen that results obtained by the present method (Superposition-Galerkin) are identical to those reported by Yu et al [15] using the traditional superposition approach. Both differ slightly from the higher order shear results tabulated by Khdeir [19].

Further results are compared in Table A.11 for square plates with the same boundary conditions, but with the ratio E_1/E_2 fixed at 40.0 and the thickness ratio ϕ_h allowed to vary. Again, results obtained by the superposition, and modified superposition methods are seen to be identical.

Finally, in Table A.12, the first six eigenvalues are tabulated for a fully clamped , CCCC, plate with thickness ratio equal to 0.1 and ratio $E_1/E_2 = 40.0$. The plate aspect ratio is allowed to take on a number of discrete values and results obtained by the traditional superposition method and the Superposition-Galerkin method introduced here are compared. It is seen that agreement between the two sets of results is excellent. The associated mode shapes of the fully clamped square plate is also presented in Figure A.7 through A.9 .

Chapter 5

Summary

5.1 Discussion and Conclusions

Two major achievements have been made in this study. They are

(1) The traditional superposition method has been used successfully to obtain the analytical solutions for the natural frequencies and mode shapes of shear deformable plates, namely, thick isotropic plates and symmetric cross-ply laminated plates, with completely free edges. The solutions obtained satisfy the governing differential equations exactly throughout the domain of the plate, and the boundary conditions can be satisfied to any desired degree of accuracy by taking more terms in the displacement solutions.

The effects of transverse shear deformation and rotary inertia have been taken into account by means of the first order shear deformation relationship as developed by Mindlin. It is found that the transverse shear deformation plays an essential role in the natural frequencies. It reduces the value of natural frequencies predicted by the classic thin plate theory. This is more pronounced in the composite plates due to the low transverse shear moduli relative to the in-plane Young's moduli.

To the author's knowledge, these solutions constitute the first accurate analytical approach to resolving these important plate vibration problems. It is expected that the tabulated eigenvalues may prove useful to designers as well as providing reference values against which future researchers may compare their results.

(2) A new modified Superposition-Galerkin method is developed to solve the free vibration problem of symmetric cross-ply plates with various combinations of clamped and simply supported edge conditions. The major difference between the modified Superposition-Galerkin method and traditional superposition method centres around the much simpler manner in which solutions are obtained for the basic building block. It is well demonstrated here that the modified Superposition-Galerkin method allows all of the advantages of the traditional superposition method to be retained while vastly simplifying the computational procedure. These computational simplifications are listed as follows:

a) The problem of reducing the set of equilibrium equations to a single sixth order ordinary

differential equation containing one dependent variable is eliminated. Because of the nature of governing differential equations, the associated characteristic equation can have numerous combinations of real, complex and/or imaginary roots, depending on the problem input parameters. Following the traditional superposition method, solutions associated with all possible combinations of such roots must be provided for in the solution procedure. The Superposition-Galerkin method eliminates the need to provide for solutions related to any combination of characteristic equation roots.

b) The formidable problem in the traditional superposition method of establishing proper expressions for the other dependent variables, once solutions for the first dependent variable are obtained, is eliminated.

c) It is known that because of the hyperbolic functions appearing in almost all possible forms of the solutions encountered when following the traditional superposition approach, serious problems related to computer over-flow, under-flow, or computational instability may be encountered. The Superposition-Galerkin method described here permits one to avoid such problems as only trigonometric functions and simple low power polynomials are involved.

d) In the generation of the eigenvalue matrix, integrals involving the same hyperbolic functions will be required when following the traditional superposition method. With the Superposition-Galerkin method only trigonometric functions and low polynomials appear

in these integrals. In fact, due to orthogonality associated with trigonometric functions, many such integrals will equal zero.

In summary, it is seen that the modified Superposition-Galerkin method leads to a vast simplification of computational procedures in comparison to the traditional superposition method. Nevertheless it is seen, as expected, that excellent agreement is encountered when results obtained by Superposition-Galerkin method are compared with those published by other researchers. It is hoped that this new modified approach is capable of handling a large family of laminated plate vibration problems.

5.2 Further Research

The present research includes isotropic thick plates with completely free edges, and symmetric cross-ply laminated plates with various clamped and simply supported edges as well as completely free edges. Further research can be extended to the following areas:

(1) Free vibration analysis of composite plates with more complicated material fabrications, such as angle-ply laminates, etc. .

(2) Free vibration analysis of composite plates with more complicated classic boundary conditions, such as elastic edge support and point supports, etc. .

(3) Free vibration analysis of composite plates subjected to in-plane forces or thermal stresses.

(4) Buckling analysis of composite plates.

(5) Free vibration and buckling analysis of composite open shells.

Reference

[1] Reissner, E. (1945). The Effect of Transverse Shear Deformation on the Bending of Elastic Plates, Journal of Applied Mechanics, Vol. 67, pp A69-77 .

[2] Mindlin, R.D. (1951). Influence of Rotary Inertia and Shear on Flexural Motions of Isotropic Elastic Plates, Journal of Applied Mechanics, Vol. 18, pp 31-38 .

[3] Gorman, D.J. (1982). Free Vibration Analysis of Rectangular Plates, Elsevier North Holland Inc. , New York .

[4] Gorman, D.J. (1978) Free Vibration Analysis of the Completely Free Rectangular Plate by the Method of Superposition, Journal of Sound and Vibration, Vol. 57, No. 3, pp 437-447 .

[5] Gorman, D.J. (1990) Accurate Free Vibration Analysis of Clamped Orthotropic Plate by the Method of Superposition, Journal of Sound and Vibration, Vol. 140, No. 3, pp 391-411 .

[6] Gorman, D.J. (1993) Accurate Free Vibration Analysis of the Completely Free Orthotropic Rectangular Plate by the Method of Superposition, Journal of Sound and Vibration, Vol. 165, No. 3, pp 409-420 .

[7] Gorman, D.J. and Ding, W. (1995) Accurate Free Vibration Analysis of the Completely

Free Rectangular Mindlin Plate, Accepted by Journal of Sound and Vibration.

[8] Gorman, D.J. and Ding, W. (1995) Accurate Free Vibration Analysis of Laminated Symmetric Cross-ply Rectangular Plates by the Superposition-Galerkin Method, Accepted by Composite Structures.

[9] Gorman, D.J. and Ding, W. (1995) The Superposition-Galerkin Method for Free Vibration Analysis of Rectangular Plates, Accepted by 15th Canadian Congress of Applied Mechanics CANCAM 95 .

[10] Ding, W. and Gorman, D.J. (1995) Free Vibration Studies of Completely Free Symmetric Cross-ply Laminated Plates, Accepted by 1995 Canadian Society for Civil Engineering Annual Conference .

[11] Gorman, D.J. and Ding, W. (1995) Free Vibration Analysis of Simply Supported-Clamped Mindlin Plates by the Superposition-Galerkin Method, Accepted by 15th Biennial Conference on Mechanical Vibration & Noise, 50th Anniversary of the ASME Design Engineering Division .

[12] Cleghorn, W.L. and Yu, S.D. (1991) Effect of Shear Deformation on Free Flexural Vibration of Clamped Rectangular Plates, ASME Machinery Dynamics and Element Vibrations, DE Vol. 36, pp 185-191 .

[13] Yu, S.D. and Cleghorn, W.L. (1992) Accurate Free Vibration Analysis of Clamped Mindlin Plates Using the Method of Superposition, Proceedings of 11th Symposium on Engineering Applications of Mechanics, University of Regina, Saskatchewan, May 11-13, pp 226-230 .

[14] Yu, S.D. and Cleghorn, W.L. (1993) Generic Free Vibration of Orthotropic Rectangular Plates with Clamped and Simply Supported Edges, Journal of Sound and Vibration, Vol.

163, pp 439-450 .

[15] Yu, S.D. , Cleghorn, W.L. and Fenton, R.G. (1994) Free Vibration and Buckling of Symmetric Cross-ply Rectangular Laminates, AIAA Journal, Vol. 11, pp 2300-2308 .

[16] Timoshenko, S. and Woinowsky-Krieger S. (1959) Theory of Plates and Shells, McGraw-Hill, New York .

[17] Jones, R.M. (1975) Mechanics of Composite Materials, Scripta and McGraw-Hill, New York .

[18] Lekhnitkii, S.G. (1968) Anisotropic Plates, Gordon and Breach Science Publishers, New York .

[19] Khdeir, A.A. (1988) Free Vibration and Buckling of Symmetric Cross-ply Laminated Plates by an Exact Method, Journal of Sound and Vibration, Vol. 126, No. 3, 447-461 .

[20] Yang, P.C. , Norris, C.H. and Stavsky Y. (1966) Elastic Wave Propagation in Heterogeneous Plates, International Journal of Solids and Structures, Vol. 2, pp 665-684.

[21] Dawe, D.J. and Raoufaeil, O.L. (1980) Rayleigh-Ritz Vibration Analysis of Mindlin Plates, Journal of Sound and Vibration, Vol. 69, pp 345-359 .

[22] Palardy, R.F. and Palazoita, A.N. (1990) Buckling and Vibration of Composite Plates Using the Levy Method, Composite Structures, Vol. 14, pp 61-86 .

[23] Dickinson, S.M. (1969) The Flexural Vibration of Rectangular Orthotropic Plates, ASME Journal of Applied Mechanics, Vol. 36, pp 101-106 .

[24] Leissa, A.W. (1969) Vibration of Plates, National Aeronautics and Space Administration,

NASA SP-160 .

[25] Leissa, A.W. (1987) Recent Studies in Plate Vibrations, 1981-1985, Part I: Classical Theory, Shock and Vibration Digest, Vol. 19, No. 2, pp 11-18 .

[26] Leissa, A.W. (1987) Recent Studies in Plate Vibrations, 1981-1985, Part II: Complicating Effects, Shock and Vibration Digest, Vol. 19, No. 3, pp 10-24 .

[27] Reddy, J.N. (1984) Energy and Variational Methods in Applied Mechanics, John Wiley, New York .

[28] Reddy, J.N. (1984) A Simple Higher Order Theory for Laminated Composite Plates, Journal of Applied Mechanics, Vol. 51, pp 745-752 .

[29] Mirsa,S. , Mallakunka, N. and Sahay, C. (1991) Shear Effects in Static and Dynamic Analysis of Orthotropic Sandwich Plates, ASME Piping Components Analysis, Piping and Structural Dynamics, PVP-Vol. 218, pp 121-125 .

[30] Li, N. and Mirza, S. (1993) Free Vibration Analysis of Antisymmetric Angle-ply Laminated Composite Plate, Proceedings of 14th Canadian Congress of Applied Mechanics, Vol. 1, pp 139-140 .

[31] Li, N. (1994) Vibration of Laminated Orthotropic Composite Plates and Shells, Ph.D. Thesis, University of Ottawa .

[32] Bert, C.W. (1979) Recent research in Composite and Sandwich Plate Dynamics, Shock and Vibration Digest, Vol. 11, No. 10, pp 13-23 .

[33] Bert, C.W. (1980) Vibration of Composite Structures, Recent Advances in Structural Dynamics, Proceeding of International Conference, University of Southeampton, Vol. 2,

pp 693-712 , Southeampton, England .

[34] Bert, C.W. (1987) Advances in Dynamics of Composite Structures, In Composite Structures, Vol. 4, pp 1-17, Elsevier Applied Science, London and New York .

[35] Vinson,J.R. and Chou, T.W. (1975) Composite Materials and Their Use in Structures, Applied Science Publishers, London .

[36] Doong, J.L. and Lee, C. (1991) Vibration and Stability of Laminated Plates Based on a Modified Plate Theory, Journal of Sound and Vibration, Vol. 152, No. 2, pp 193-201 .

[37] Liew, K.M. , Hung, K.C. and Lim, M.K. (1993) A continuum Three-Dimensional Vibration Analysis of Thick Rectangular Plates, International Journal of Solids and Structures, Vol. 30, No. 24, pp 3357-3379 .

Appendix I

Illustrative Figures

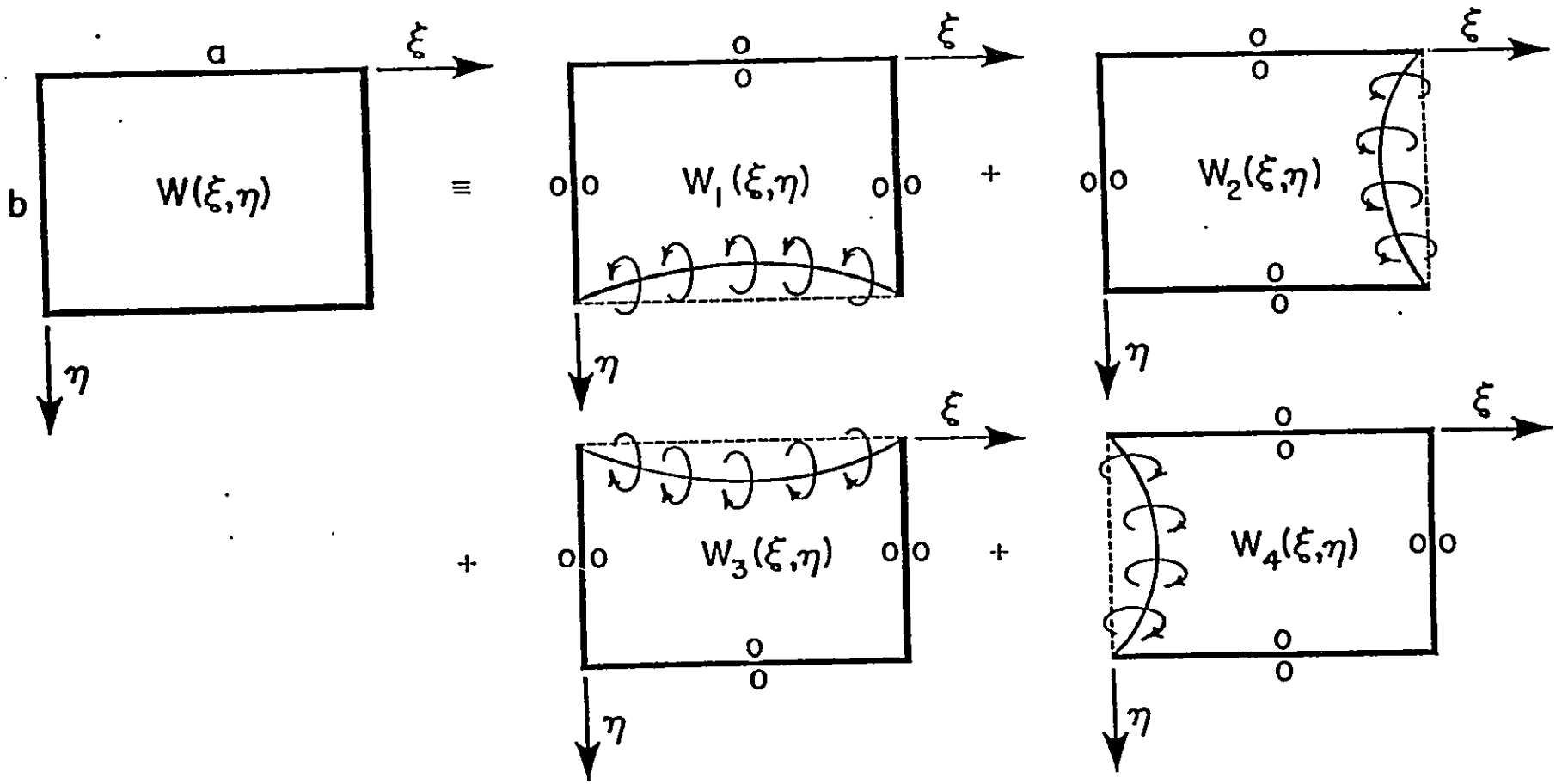

Figure 1 Schematic representation of forced vibration solutions (building blocks) utilized in free vibration analysis of completely free shear deformable plates

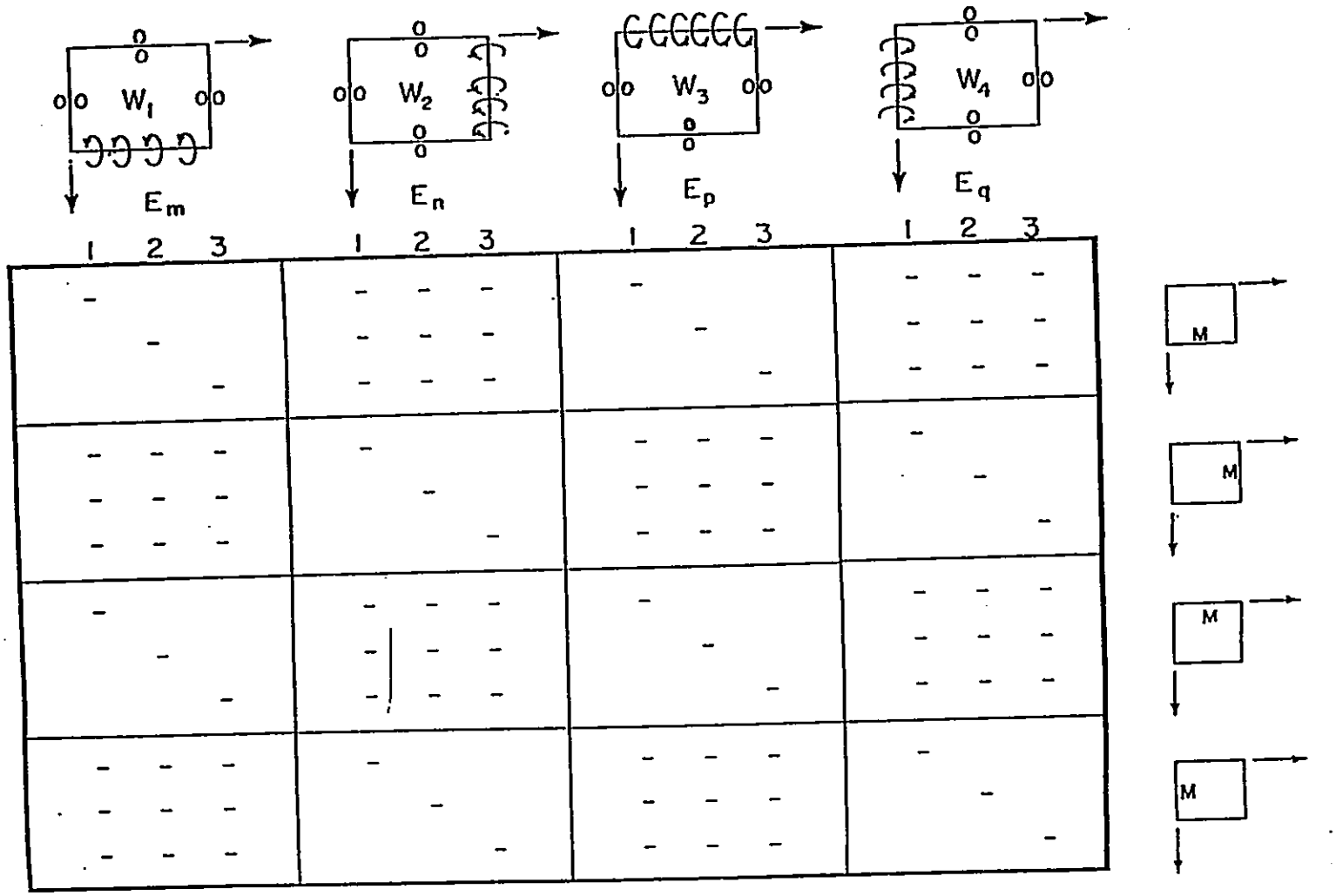

Figure 2 Schematic representation of eigenvalue matrix generated in free vibration analysis of completely free shear deformable plates

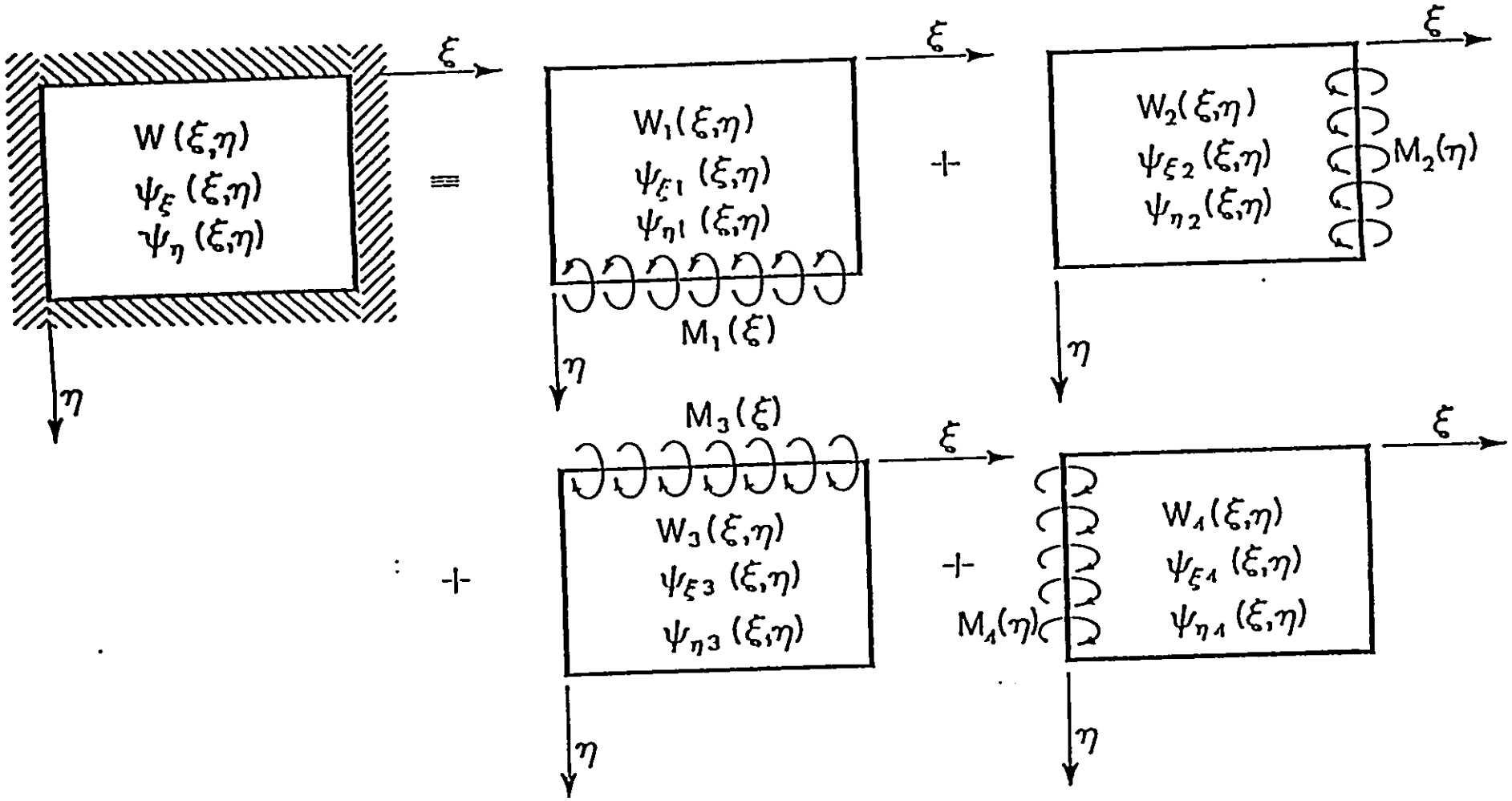

Figure 3 Schematic representation of forced vibration solutions (building blocks) superimposed in order to solve the free vibration problem of fully clamped symmetric cross-ply laminated plates

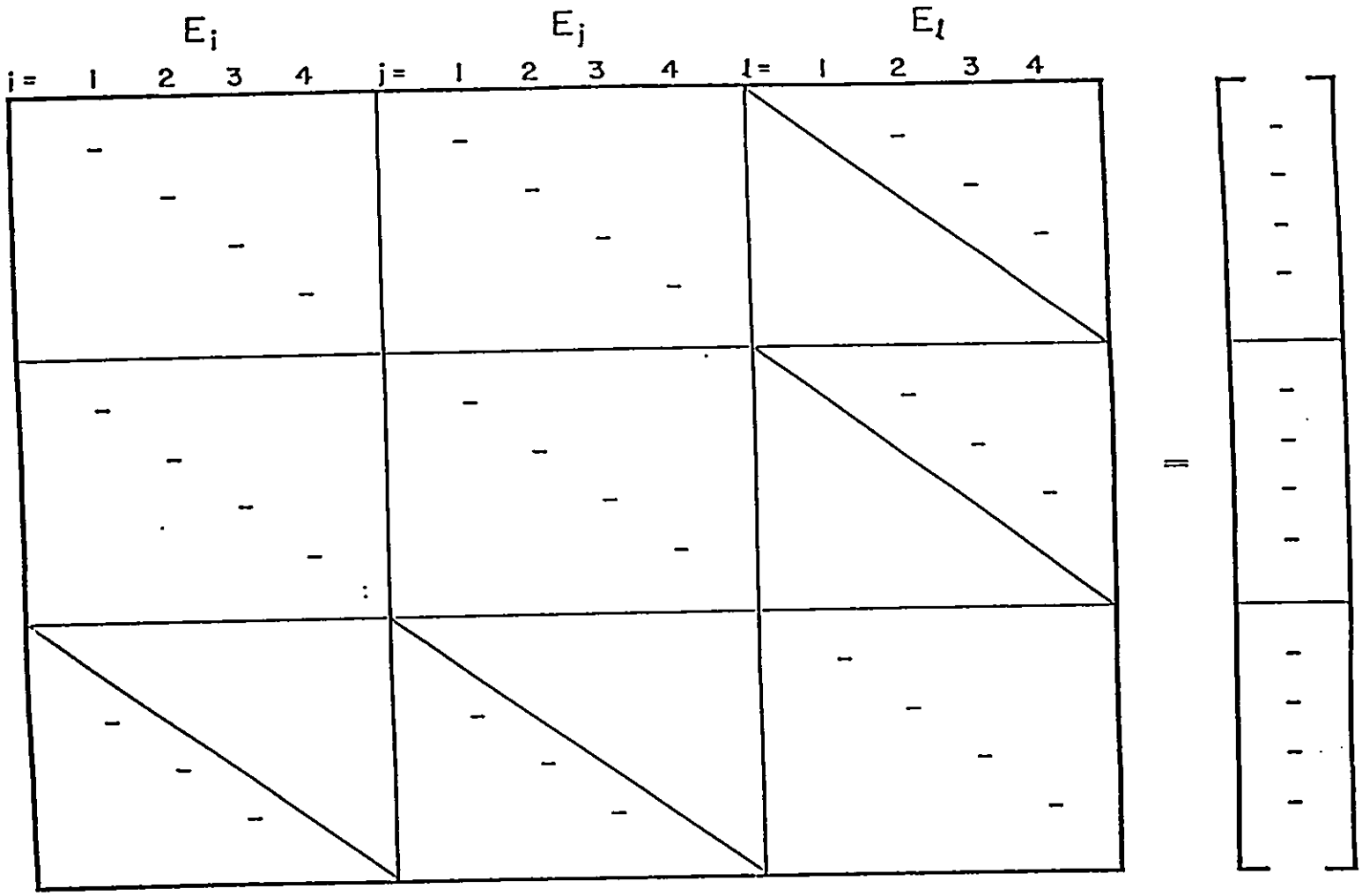

Figure 4 Schematic representation of system of simultaneous non-homogeneous algebraic equations relating coefficients employed in Galerkin Method

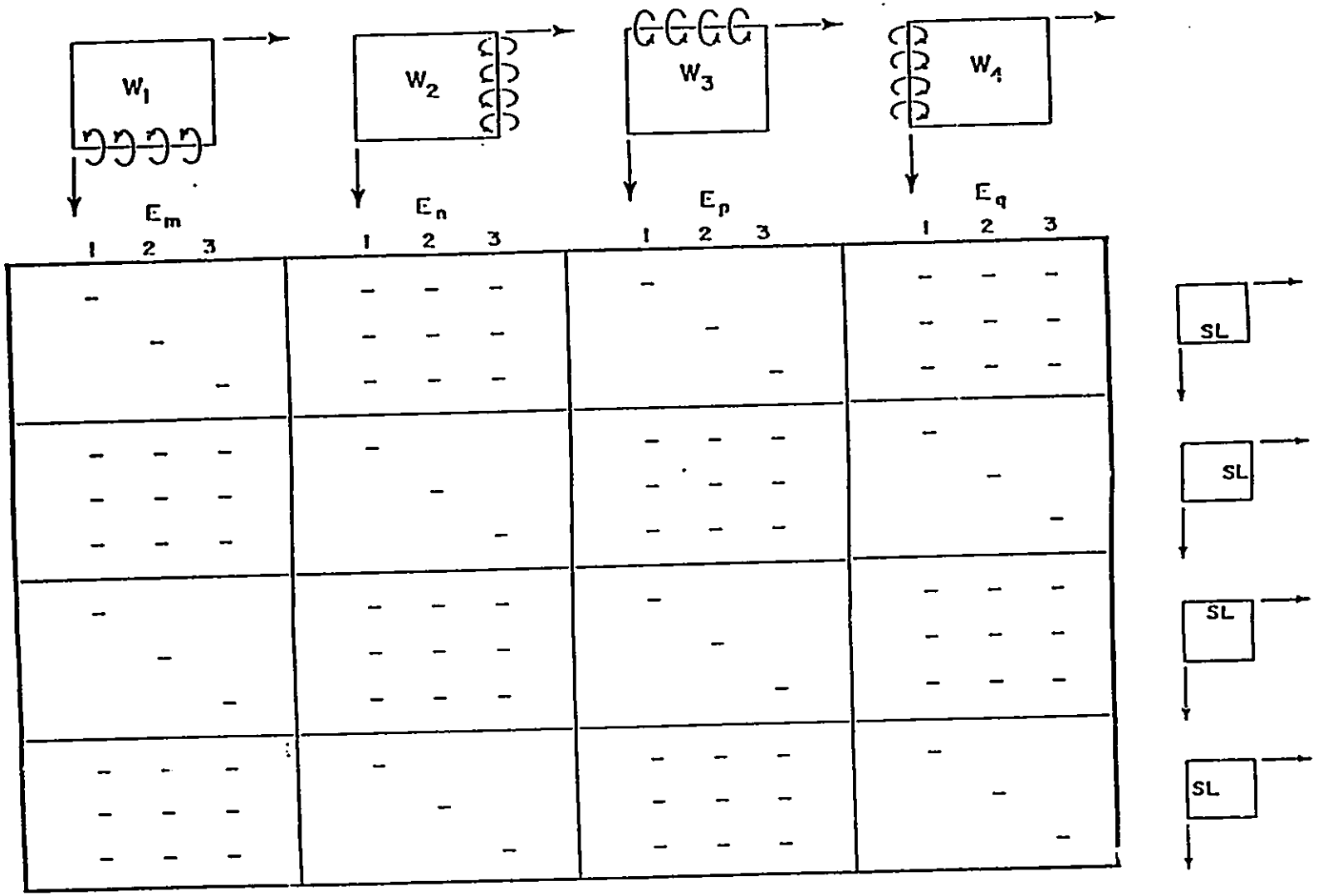

Figure 5 Schematic representation of eigenvalue matrix generated for solving the free vibration problem of fully clamped symmetric cross-ply laminated plates

Appendix II

Computed Eigenvalues

and Associated Mode Shapes

Table A.1 Eigenvalues computed for completely free isotropic thick plates ($\nu = 0.333$; $\kappa^2 = 0.8601$; $\phi = 1.0$)

MODE	T.P.T.	TYPE	ϕ_h					
			0.01	0.02	0.04	0.06	0.08	0.10
1	13.17	ASYM	13.12	13.06	12.92	12.78	12.61	12.44
2	19.22	SYM	19.22	19.20	19.11	18.98	18.80	18.59
3	24.42	SYM	24.41	24.37	24.25	24.05	23.77	23.45
4	34.23	S-A	34.09	33.91	33.44	32.85	32.17	31.40
5	60.92	S-A	60.85	60.63	59.82	58.57	56.97	55.14
6	62.76	SYM	62.40	61.91	60.59	58.92	56.99	54.90
7	68.12	ASYM	67.82	67.36	66.00	64.18	62.01	59.63
8	76.96	ASYM	76.72	76.25	74.78	72.70	70.19	67.43
9	104.2	S-A	103.5	102.5	99.54	95.66	91.25	86.61
10	116.4	SYM	116.2	115.4	112.4	108.1	103.1	97.61

Table A.2 Eigenvalues computed for completely free isotropic thick plates ($\nu = 0.333$; $\kappa^2 = 0.8601$; $\phi = 1.25$)

MODE	T.P.T.	TYPE	ϕ_h					
			0.01	0.02	0.04	0.06	0.08	0.10
1	10.52	ASYM	10.48	10.44	10.34	10.24	10.12	10.00
2	13.42	SYM	13.42	13.40	13.37	13.30	13.21	13.10
3	22.38	SYM	22.37	22.34	22.23	22.06	21.83	21.55
4	25.45	S-A	25.35	25.23	25.08	24.85	24.54	24.17
5	29.87	A-S	29.77	29.64	29.30	28.86	28.34	27.74
6	39.42	A-S	39.38	39.28	38.93	38.39	37.67	36.83
7	49.64	ASYM	49.43	49.15	48.38	47.34	46.09	44.69
8	50.76	SYM	50.49	50.15	49.24	48.08	46.74	45.26
9	60.72	S-A	60.64	60.43	59.61	58.36	56.77	54.94
10	69.08	ASYM	68.87	68.49	67.28	65.58	63.49	61.16

Table A.3 Eigenvalues computed for completely free isotropic thick plates ($\nu = 0.333$; $\kappa^2 = 0.8601$; $\phi = 1.5$)

MODE	T.P.T.	TYPE	ϕ_h					
			0.01	0.02	0.04	0.06	0.08	0.10
1	8.732	ASYM	8.701	8.668	8.597	8.517	8.431	8.338
2	9.412	SYM	9.411	9.405	9.385	9.352	9.308	9.253
3	20.23	S-A	20.15	20.06	19.85	19.60	19.31	18.98
4	22.13	SYM	22.12	22.09	21.99	21.82	21.60	21.32
5	25.25	A-S	25.20	25.14	24.94	24.66	24.30	23.89
6	29.75	A-S	29.70	29.62	29.36	29.01	28.56	28.03
7	37.63	ASYM	37.49	37.31	36.81	36.15	35.37	34.49
8	43.28	SYM	43.09	42.83	42.15	41.28	40.26	39.13
9	52.24	SYM	53.15	52.98	52.35	51.37	50.12	48.67
10	59.52	S-A	59.41	59.14	58.26	56.97	55.35	53.52

Table A.4 Eigenvalues computed for completely free isotropic thick plates (ν = 0.333 ; κ^2 = 0.8601 ; ϕ = 2.0)

MODE	T.P.T.	TYPE	ϕ_h					
			0.01	0.02	0.04	0.06	0.08	0.10
1	5.312	SYM	5.309	5.307	5.300	5.290	5.275	5.257
2	6.492	ASYM	6.472	6.450	6.401	6.347	6.289	6.227
3	14.34	S-A	14.28	14.23	14.11	13.96	13.79	13.60
4	14.77	A-S	14.76	14.74	14.69	14.60	14.48	14.34
5	21.90	SYM	21.89	21.87	21.76	21.60	21.38	21.10
6	24.98	ASYM	24.89	24.79	24.52	24.19	23.79	23.34
7	25.81	A-S	25.76	25.69	25.48	25.19	24.84	24.42
8	29.52	SYM	29.49	29.43	29.21	28.88	28.45	27.93
9	35.70	SYM	35.57	35.41	34.97	34.38	33.69	32.90
10	39.54	S-A	39.42	39.23	38.71	38.02	37.18	36.24

Table A.5 Eigenvalues computed for completely free isotropic thick plates ($\nu = 0.333$; $\kappa^2 = 0.8601$; $\phi = 2.5$)

MODE	T.P.T.	TYPE	ϕ_h					
			0.01	0.02	0.04	0.06	0.08	0.10
1	3.396	SYM	3.396	3.395	3.392	3.388	3.382	3.374
2	5.156	ASYM	5.141	5.124	5.087	5.046	5.003	4.956
3	9.456	A-S	9.453	9.446	9.442	9.385	9.336	9.276
4	11.10	S-A	11.06	11.02	10.93	10.83	10.71	10.59
5	18.45	SYM	18.44	18.41	18.30	18.08	17.84	17.56
6	18.60	ASYM	18.54	18.47	18.33	18.19	18.02	17.80
7	22.45	SYM	22.44	22.41	22.31	22.14	21.91	21.63
8	24.24	A-S	24.20	24.15	23.97	23.73	23.42	23.08
9	28.34	S-A	28.25	28.14	27.83	27.43	26.95	26.40
10	31.14	SYM	31.04	30.92	30.58	30.13	29.59	28.97

Table A.6 Eigenvalues computed for completely free isotropic thick plates ($\nu = 0.333$; $\kappa^2 = 0.8601$; $\phi = 3.0$)

MODE	T.P.T.	TYPE	ϕ_h					
			0.01	0.02	0.04	0.06	0.08	0.10
1	2.357	SYM	2.356	2.356	2.354	2.352	2.349	2.345
2	4.276	ASYM	4.261	4.247	4.217	4.184	4.149	4.112
3	6.556	A-S	6.555	6.551	6.539	6.521	6.497	6.467
4	9.052	S-A	9.022	8.991	8.921	8.843	8.756	8.661
5	12.92	SYM	12.91	12.90	12.86	12.79	12.70	12.59
6	14.80	ASYM	14.75	14.70	14.57	14.42	14.25	14.06
7	21.10	A-S	21.08	21.05	20.93	20.75	20.52	20.24
8	21.94	S-A	21.88	21.79	21.58	21.31	21.00	20.64
9	22.19	SYM	22.18	22.15	22.05	21.88	21.65	21.38
10	24.31	A-S	24.29	24.24	24.09	23.86	23.57	23.22

Table A.7 **Comparison of eigenvalues, $\lambda^2 = \omega a^2\sqrt{\rho/E_2h^3}$, for orthotropic plates with $D_x/D_y = 4.0$, $H = \sqrt{D_xD_y}$, $\sqrt{\nu_{12}\nu_{21}} = 0.25$. T.P.T. and P indicate plate theory [6] and the present Theory, respectively. Parameters ϕ_h was set equal to 0.01 .**

MODE	PLATE ASPECT RATIO $\phi = b/a$											
	1.0		1.25		1.50		2.0		2.50		3.0	
	T.P.T.	P	T.P.T.	P	T.P.T.	P	T.P.T.	P	T.P.T.	P	T.P.T.	P
1	5.841	5.828	4.150	4.148	2.881	2.881	1.620	1.620	1.036	1.036	0.7191	0.7191
2	6.466	6.465	4.646	4.637	3.852	3.844	2.860	2.860	2.280	2.280	1.893	1.890
3	13.28	13.28	10.35	10.32	8.374	8.357	6.061	6.049	4.749	4.739	3.904	3.897
4	13.55	13.51	11.52	11.47	13.15	13.14	8.823	8.821	5.698	5.646	3.916	3.916
5	25.31	25.24	13.23	13.23	14.30	14.26	9.910	9.890	7.582	7.568	6.142	6.131
6	28.12	28.03	18.32	18.28	15.89	15.88	13.30	13.29	10.94	10.92	8.704	8.691

Table A.8 **First four eigenvalues, $\lambda^2 = \omega a^2\sqrt{\rho/E_2h^3}$, for completely free $0^0/90^0/0^0$ symmetric cross-ply plates. Material properties as given by Khdeir[19].** ($\phi \geq 1$, $\phi_h = 0.1$)

MODE	PLATE ASPECT RATIO b/a		
	1.0	1.5	2.0
1	4.873	3.258	2.431
2	9.662	4.399	2.497
3	13.33	7.775	5.479
4	24.57	11.65	6.723

Table A.9 **First four eigenvalues, $\lambda^2 = \omega a^2\sqrt{\rho/E_2h^3}$, for completely free $0^0/90^0/0^0$ symmetric cross-ply plates. Material properties as given by Khdeir[19].** ($1/\phi \geq 1$, ϕ_h=0.1)

MODE	INVERSE OF PLATE ASPECT RATIO b/a		
	1.0	1.5	2.0
1	4.873	3.186	2.325
2	9.662	9.198	7.384
3	13.33	10.76	8.071
4	24.57	13.13	8.673

Table A.10 **Comparison of computed eigenvalues, $\lambda^2 = \omega a^2\sqrt{\rho/E_2 h^3}$, for square symmetric cross-ply plates ($\phi_h = 0.1$). HSDPT and HSDT results taken from publication of Khdeir [19].**

SOURCE	E_1/E_2 (SSSC)			E_1/E_2 (SCSC)		
	20	30	40	20	30	40
HSDPT	15.036	16.458	17.427	18.124	19.448	20.315
HSDT	14.888	16.203	17.069	17.727	18.830	19.500
Yu et al	15.059	16.430	17.336	18.017	19.187	19.898
Present	15.059	16.430	17.336	18.017	19.187	19.898

Table A.11 **Comparison of computed eigenvalues, $\lambda^2 = \omega a^2\sqrt{\rho/E_2 h^3}$, for square symmetric cross-ply plates ($E_1/E_2 = 40$). HSDPT and HSDT results taken from publication of Khdeir [19].**

SOURCE	$1/\phi_h$ (SSSC)			$1/\phi_h$ (SCSC)		
	5	10	15	5	10	15
HSDPT	11.156	17.427	21.325	12.333	20.315	26.183
HSDT	10.576	17.069	21.131	11.164	19.500	25.652
Yu et al	10.768	17.336	21.373	11.411	19.898	26.072
Present	10.768	17.336	21.373	11.411	19.898	26.072

Table A.12 **First six computed Eigenvalues, $\lambda^2 = \omega a^2\sqrt{\rho/E_2 h^3}$, for symmetric cross-ply laminated plates with fully clamped boundary conditions. ($\phi_h = 0.1$, $E_1/E_2 = 40.0$)**

MODE	PLATE ASPECT RATIO $\phi = b/a$									
	2.0		4/3		1.0		2/3		1/2	
	Yu et al	Present	Yu et al	Present	Yu et al	Present	Yu et al	Present	Yu et al	Present
1	19.48	19.48	20.09	20.09	21.45	21.45	26.87	26.87	35.18	35.18
2	20.50	20.50	23.92	23.92	29.98	29.98	43.61	43.61	49.23	49.23
3	23.12	23.12	31.91	31.91	40.39	40.39	47.11	47.12	67.03	67.03
4	27.69	27.68	39.63	39.63	44.50	44.50	58.64	58.64	68.57	68.57
5	34.02	34.03	41.92	41.92	45.78	45.78	64.63	64.63	75.70	75.70
6	39.27	39.27	43.13	43.13	56.60	56.61	74.40	74.40	89.41	89.41

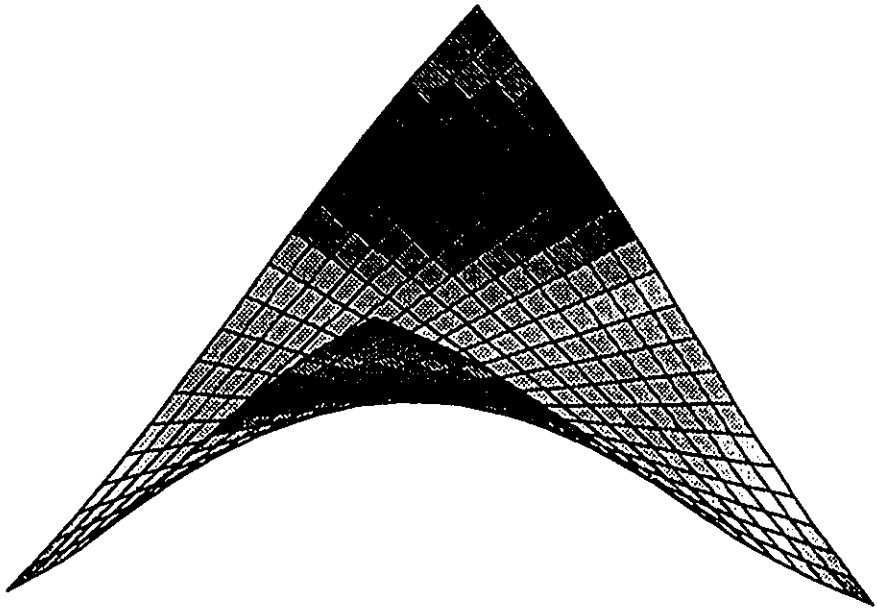

Figure A.1 First mode shape of completely free thick isotropic square plates by the traditional superposition method ($\phi_h = 0.1$, $\lambda^2 = 12.44$)

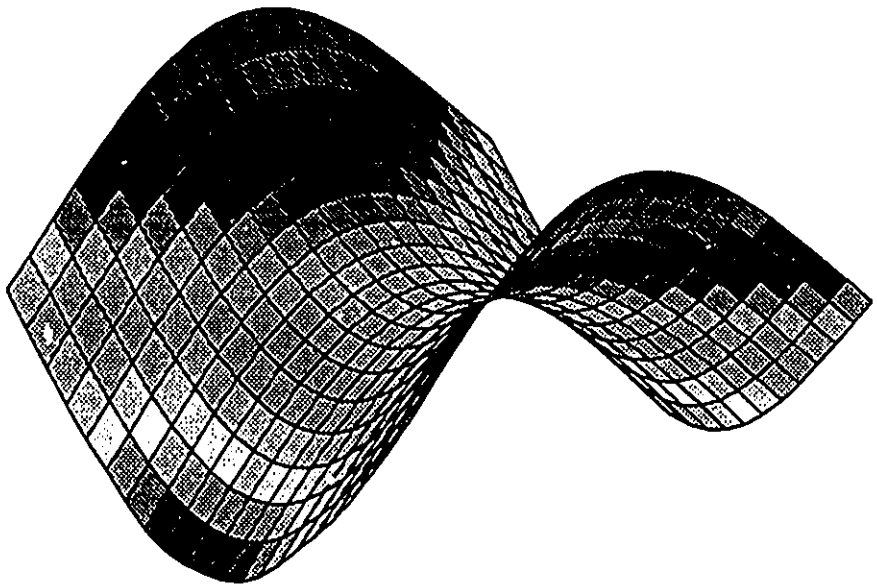

Figure A.2 Second mode shape of completely free thick isotropic square plates by the traditional superposition method ($\phi_h = 0.1$, $\lambda^2 = 18.58$)

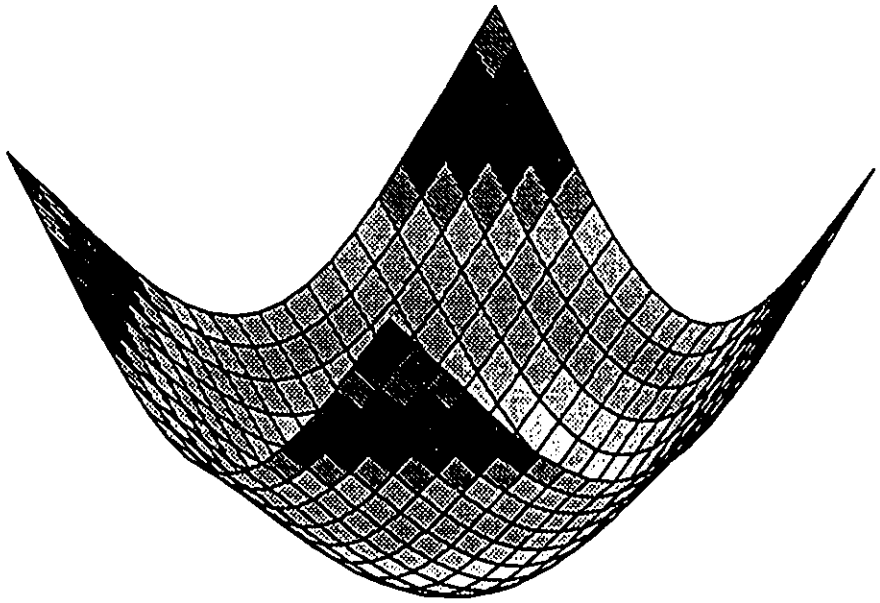

Figure A.3 Third mode shape of completely free thick isotropic square plates by the traditional superposition method ($\phi_h = 0.1$, $\lambda^2 = 23.45$)

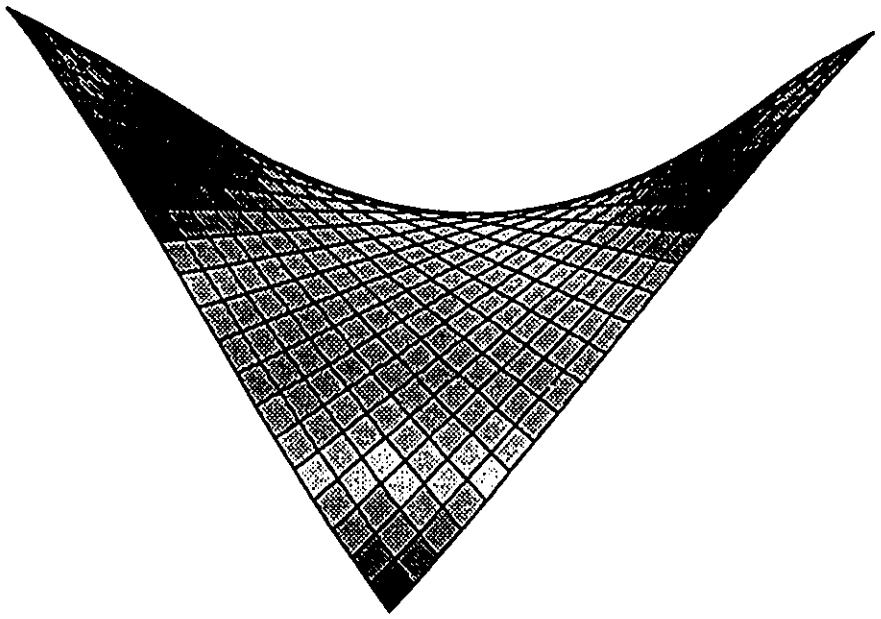

Figure A.4 First mode shape of completely free symmetric cross-ply square plates by the traditional superposition method (ϕ_h = 0. 1 , λ^2 = 4. 873)

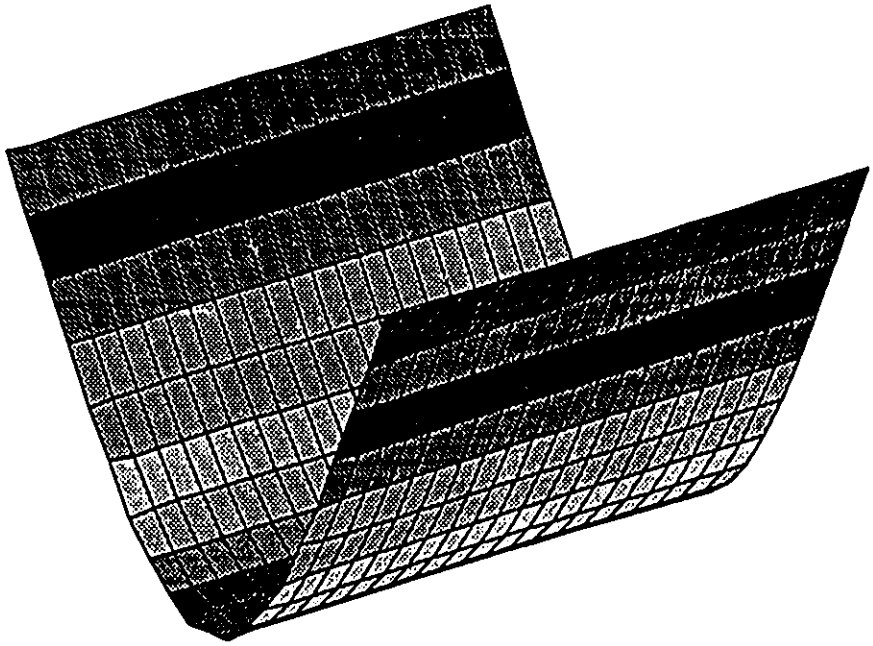

Figure A.5 Second mode shape of completely free symmetric cross-ply square plates by the traditional superposition method ($\phi_h = 0.1$, $\lambda^2 = 9.662$)

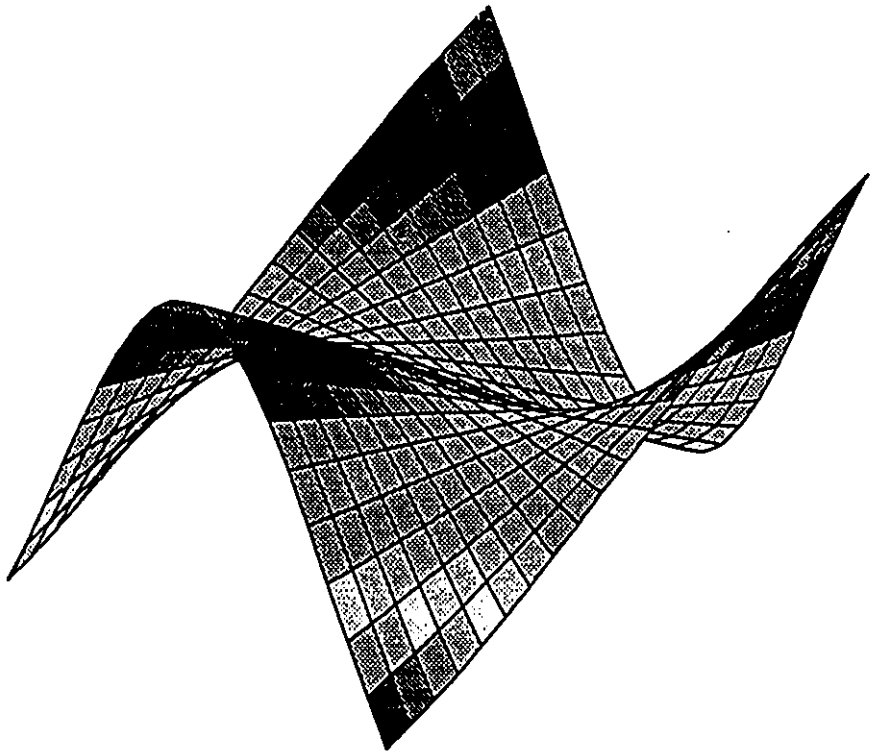

Figure A.6 Third mode shape of completely free symmetric cross-ply square plates by the traditional superposition method ($\phi_h = 0.1$, $\lambda^2 = 13.33$)

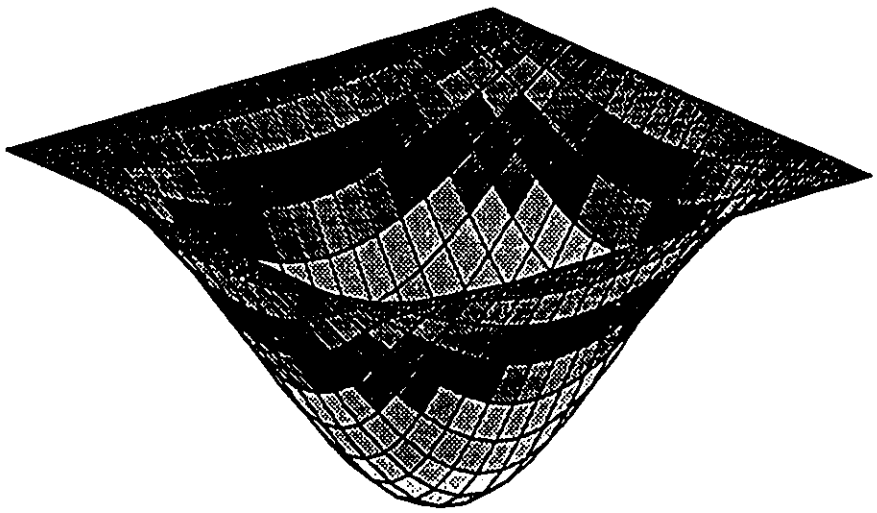

Figure A.7 First mode shape of fully clamped symmetric cross-ply square plates by the Superposition-Galerkin method ($\phi_h = 0.1$, $\lambda^2 = 21.45$)

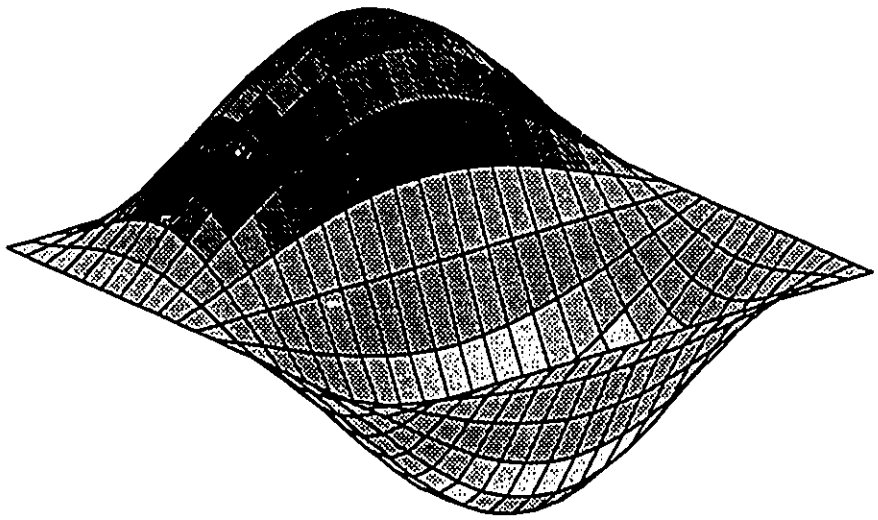

Figure A.8 Second mode shape of fully clamped symmetric cross-ply square plates by the Superposition-Galerkin method ($\phi_h = 0.1$, $\lambda^2 = 29.98$)

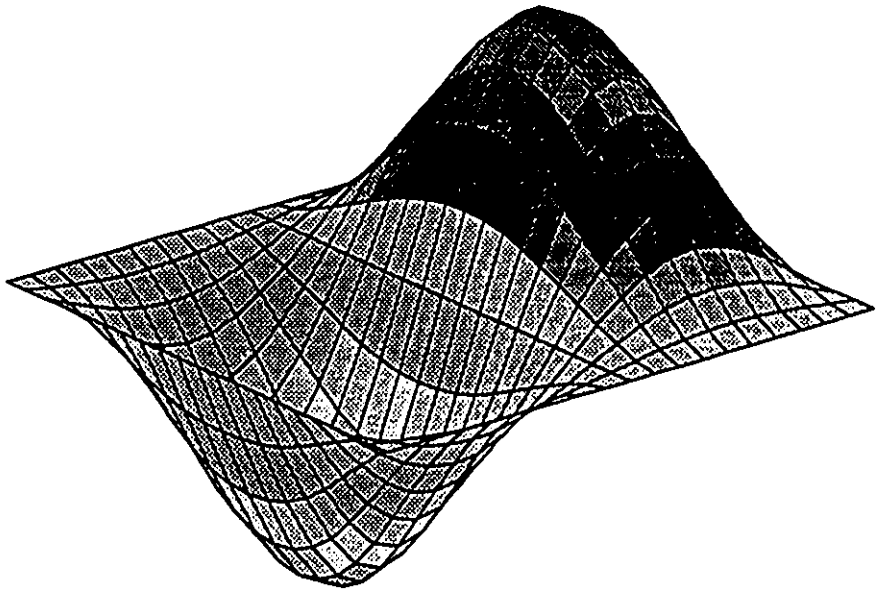

Figure A.9 Third mode shape of fully clamped symmetric cross-ply square plates by the Superposition-Galerkin method ($\phi_h = 0.1$, $\lambda^2 = 40.39$)